BAYESIAN SPATIAL AND SPATIO-TEMPORAL MODELS FOR SKEWED AREAL COUNT DATA

BENARD CHERUIYOT TONUI

DOCTOR OF PHILOSOPHY
(Applied Statistics)

JOMO KENYATTA UNIVERSITY OF AGRICULTURE AND TECHNOLOGY

2021

Bayesian Spatial and Spatio-temporal Models for Skewed Areal Count Data

Benard Cheruiyot Tonui

A Thesis Submitted in Partial Fulfillment of the Requirements for the Degree of Doctor of Philosophy in Applied Statistics of the Jomo Kenyatta University of Agriculture and Technology

2021

DECLARATION

This thesis is my original work and has not been presented for a degree in any other University.

Signature: .... Date: ....

Benard Cheruiyot Tonui

This thesis has been submitted for examination with our approval as University Supervisors.

Signature: .... Date: ....

Prof. Samuel Mwalili, PhD

JKUAT, Kenya

Signature: .... Date: ....

Dr. Anthony Wanjoya, PhD

JKUAT, Kenya

DEDICATION

To my sons Felix, Collins, Alex and Arnold

ACKNOWLEDGEMENTS

I would like to acknowledge very important persons who, before and during the course of my PhD, have contributed through diverse ways to the success of this thesis. First of all, I will credit God for being my guide, providing renewed strength each day throughout my entire life.

I wish to thank my supervisors Prof. Samuel Mwalili and Dr. Anthony Wanjoya of JKUAT for the wonderful years of great supervision. Your guidance, support, suggestions and contributions are beyond par. It has been a delightful privilege and honor to have learnt from and been mentored by such great minds. I am forever grateful. In a special way, I am grateful to all the members of the Statistics and Actuarial Science department, JKUAT, for the guidance I received at all the presentations, towards my progress, organized through the department.

I also appreciate and acknowledge the support of my employer, University of Kabianga, through the study leave to enable me conduct my research and finalize on data analysis and the thesis write up. In particular, I would like to thank the Head of Mathematics & Computer Science department, Dr. D. Adicka, for allowing me to proceed on the study leave. I am also thankful to Prof. M. Oduor, the Dean School of Science and Technology, who yearned to see the successful completion of my work. The support of my colleague, Dr. R. Langat, cannot go unnoticed as he has mentored me since my high school days and later on introducing me to the field of Statistics.

This thesis will not have been possible without the support of my family. My very special thanks go to my beloved wife, Caro, for the inspirational and endless care and for the many sacrifices during the entire period of my PhD studies. To my elder brother, Kipkoech Tonui, I thank you so much for the financial support and seeing me through my early education. Thank you for motivating me to pursue a career in mathematics; it has been a very interesting and inspiring journey. I am pleased with the number of opportunities that have come my way ever since. Finally, to my dearest mum, Elizabeth, I am grateful for your unwavering efforts and for sacrificing everything to ensure that I pursue my dream.

TABLE OF CONTENTS

LIST OF TABLES

LIST OF FIGURES

LIST OF APPENDICES

ABBREVIATIONS AND ACRONYMS

BYM	Besag, York and Molli´e
CAR	Conditional Autoregressive
CH	Correlated Heterogeneity
CON	Convolution
DIC	Deviance Information Criterion
EB	Empirical Bayes
FB	Fully Bayes
GLM	Generalized Linear Models
GLMM	Generalized Linear Mixed Models
GMRF	Gaussian Markov Random Field
GOF	Goodness-of-fit
GPS	Global Positioning System
HIV	Human Immunodeciency Virus
ICAR	Intrinsic Conditional Autoregressive
ICAR CH	Intrinsic Conditional Autoregressive Correlated Heterogeneity
ICAR CON	Intrinsic Conditional Autoregressive Convolution
INLA	Integrated Laplace Approximation
KEMRI	Kenya Medical Research Institute
KNBS	Kenya National Bureau of Statistics

MCMC	Markov chain Monte Carlo
MSPE	Mean Squared Predictive Error
NACC	National AIDS Control Council
NASCOP	National AIDS and STI Control Programme
NCAPD	National Council for Population and Development
pCAR	Proper Conditional Autoregressive
pCARCOM	Proper Conditional Autoregressive Combined
pD	Effective number of parameters
PG	Poisson-Gamma
PLN	Poisson-lognormal
PLHIV	People Living with HIV
PLSN	Poisson-log-skew-normal
PLST	Poisson-log-skew-t
PLT	Poisson-log-t
PMTCT	Prevention of Mother to Child Transmission
LCAR	Leroux Conditional Autoregressive
RR	Relative Risk
SIR	Standardized Incidence Rate
SN	Skew-normal
ST	Skew-t
STCAR	Skew-t Conditional Autoregressive
STCARCOM	Skew-t Conditional Autoregressive Combined
UH	Uncorrelated Heterogeneity

ABSTRACT

Disease mapping models have found wide range of applications to epidemiology and public health. These models typically extend from generalized linear models (GLM) and are usually implemented using a Bayesian approach. Most of the disease mapping models incorporate random effects that assume either a Gaussian exchangeable prior for the spatially unstructured heterogeneity or the popular Gaussian CAR priors for the spatially structured variability. However, this Gaussian assumption is often violated since random effects can be skewed. This thesis proposed models that relax the usual normality assumption on the spatially unstructured random effect by using skew normal and skew-t distributions. In the analysis of 2016 HIV and AID data in Kenya, it was found out that models whose unstructured random effects follow asymmetric skewed distributions perform better than models with corresponding symmetric distributed unstructured random effects. Classical random-effects models for count data includes the Poisson-gamma model, that utilizes the conjugate feature between the Poisson and Gamma distributions to attain closed-form posterior distribution but accounts only for overdispersion or extra variation, and the Gaussian conditional autoregressive (CAR) models, that model spatial correlation but does not have a closed-form posterior distribution. This thesis also considers an alternative model that combines a Poisson-gamma model with a spatially structured skew-t random effect in the same model thus accounting for the extra variability, spatial correlation and skewness in the data. In the analysis of 2016 Kenya HIV and AIDS data, the skew-t spatial combined random effects model was found to provide a better alternative to the classical disease mapping models. Simulation studies also show that the proposed models perform better than the classical disease mapping models. To model spatio-temporal variation, this thesis considered Leroux CAR (LCAR) prior for spatial random effect and implemented Bayesian analysis using integrated nested Laplace approximations (INLA). In the analysis of spatio-temporal variation of HIV and AIDS in Kenya for the period 2013–2016, it was found out that counties located in the Western region of Kenya show significantly higher HIV and AIDS risks as compared to the other counties.

CHAPTER ONE

INTRODUCTION

1.1 Overview of Spatial and Spatio-temporal data

Spatial and spatio-temporal data have become more accessible in the recent past mainly due to the availability of computational tools which has made collection of real-time data from sources like GPS and satellites possible (Lawson and Lee, 2017; Arab, 2015). Therefore, the researchers in various fields like epidemiology, ecology, climatology and social sciences frequently encounter geo-referenced data which capture information about space and also possibly time. Spatial and spatio-temporal modeling play a very important role in various studies which include disease mapping. Hierarchical spatial and spatio-temporal models often offer a flexible approach for modeling spatially correlated and temporally dependent count data. This thesis considers Bayesian hierarchical spatial and spatio-temporal disease mapping models and their extensions with application to modeling HIV and AIDS data.

Data whose location in space is known (i.e, geographically referenced) are referred to as spatial data. Banerjee *et al.* (2015) defined spatial data as realizations of stochastic process indexed by space

$$Y(\mathbf{s}) = \{y(\mathbf{s}), \mathbf{s} \in \mathcal{D}\} \tag{1.1}$$

where $\mathcal{D} \subset \mathbb{R}^d$ ($d = 2$ or 3) with spatial coordinates $\mathbf{s} = (s_1, ..., s_d)'$.

Spatial stochastic processes vary in the plane with $d = 2$ and the coordinates are given by the ordered pair $\mathbf{s} = (x, y)'$ (i.e, longitude and latitude). The spatial process can be easily extended to the spatio-temporal case including a time component so that the data are now defined by a process indexed by a set on a space-time manifold with $d = 3$ and their coordinates are given by $\mathbf{s} = (x, y, t)'$. That is, for observations made at n spatial areas or locations and at time point t;

$$Y(s,t) = \left\{y(s,t), (s,t) \in D \subset \mathbb{R}^3\right\} \tag{1.2}$$

In general, stochastic processes with $d \geq 2$ are referred to as random fields.

Spatial data sets can be classified into one of the following three basic types:

(i) *Areal or lattice data:* This is where data values $y(s_1), ..., y(s_n)$ are observations associated with a fixed number of areal units (area objects) that may form a regular lattice, as in the case of remotely sensed images, or be a set of irregular areas or zones based on administrative boundaries, such as districts, counties, census zones, regions or even countries. Often $y(\mathbf{s})$ represents a suitable summary like the number of observed cases in each area and is referred to as *areal or lattice data*. In this case, the interest is usually on mapping or smoothing an outcome over the domain $\mathcal{D}$.

(ii) *Point-Referenced or geostatistical data:* This relates to variables which change continuously in space and whose observations have been sampled at a predefined and fixed set of point locations. For example, a realization of the air pollution process $y(\mathbf{s})$ in which a collection of air pollutant measurements are obtained by monitors located in the set $(s_1, s_2, \cdots, s_n)$ of n points (rather than areas) is often referred to as *point-referenced or geostatistical data*.

(iii) *Spatial Point pattern data:* This refers to data set consisting of a series of point locations in some study region, at which events of interest have occurred, such as cases of a disease or incidence of a type of crime. Here, $y(\mathbf{s})$ represents the occurrence or not of an event such that it takes the values 0 or 1 and locations $\mathbf{s} \in \mathbb{R}^d$ are random. Such data are referred to as *Spatial Point pattern data*

For exhaustive documentation of each type of spatial data and comprehensive theoretical foundations, see for example Banerjee *et al.* (2015), Gelfand *et al.* (2010) and Cressie (1993).

If the data considered are available at the area level and consist of aggregated counts of outcomes and covariates, typically disease mapping and/or ecological regression can be specified (Richardson, 2003; Lawson *et al.*, 2009).

1.2 Disease Mapping

Disease mapping is the study of the geographical or spatial distribution of health outcomes. In disease mapping, the objective of analysis is usually to estimate the true relative risk of a disease of interest across a geographical study area. Disease mapping is useful for several purposes such as health services resource allocation, disease atlas construction, detection of clustering of a disease and in formulation of hypotheses about disease aetiology. Several statistical reviews on disease mapping have been done (Hu *et al.*, 2020; Coly *et al.*, 2019; Riebler *et al.*, 2016; Wakefield, 2007; Lawson, 2001; Bithell, 2000).

1.3 Statement of the Problem

Methods for mapping diseases has progressed considerably in recent years. These models basically, utilize random effects that are partitioned into spatially correlated and uncorrelated components. In the analysis of areal data, the spatially uncorrelated random effects are mainly modelled using a Gaussian exchangeable prior. In practice, however, epidemiological or disease data is often observed to be non-normal, potentially limiting the degree to which Gaussian random effects models can be appropriately fit to data. This thesis, thus, considered models that allow for random effect distributions that are highly skewed or have excess kurtosis. Therefore, we investigated disease mapping models in which the spatially unstructured heterogeneity is modelled using skew-normal (SN) or skew-t (ST) distributions while spatially structured heterogeneity is modelled with a skew-t spatial random effect distribution. In addition, to account for overdispersion in spatially correlated and also possibly skewed data, this thesis considered an alternative model that combines a Poisson-gamma model with a spatially structured skew-t random effect in the same model; thus, accounting for the extra variability, spatial correlation and skewness in the data. This thesis also considered more efficient spatio-temporal models for such data. This was necessitated by the availability of data recorded for different regions over a period of time. This involved use of the recently developed strategy for Bayesian inference called integrated nested Laplace Approximation (INLA); INLA allows fairly complex models to be fit much faster than the popular Markov chain Monte Carlo (MCMC) algorithms.

1.4 Objectives of the Study

1.4.1 General Objective

The main objective of this study is to develop flexible Bayesian spatial and spatio-temporal hierarchical disease mapping models for skewed areal count data.

1.4.2 Specific Objectives

The specific objectives in this study are to:

(i) develop a disease mapping model with skew-random effect distributions for the spatially unstructured random effects.

(ii) develop a Poisson-gamma model for spatially correlated and overdispersed skew count data.

(iii) carry out simulation studies to assess the performance of the proposed models.

(iv) determine the spatio-temporal variation of HIV and AIDS infections in Kenya.

1.5 Justification of the Study

The disease mapping models developed in this study play an important role in addressing the spatio-temporal variation of HIV and AIDS in Kenya. Through these models, the disease hot spot areas with extreme risks are identified. This is crucial in decision-making related to health surveillance, which include optimal allocation of resources for mitigation and prevention of disease in the affected areas.

1.6 Kenya HIV and AIDS data set

In Kenya the HIV and AIDS data is obtained from the national surveys: the Kenya Demographic and Health Survey of 2003 (CBS and MOH, 2004), the Kenya AIDS Indicator Survey 2007 (NASCOP, 2009), the Kenya Demographic and Health Survey of 2008/9 (KNBS, 2010), the Kenya AIDS Indicator Survey 2012 (NASCOP, 2014), the Kenya Demographic and Health Survey of 2014 (KNBS *et al.*, 2015) and the Kenya Demographic and Health Survey of 2017 (NASCOP *et al.*, 2017). In addition, the Kenya HIV and AIDS data is supplemented by HIV testing among pregnant women at Prevention of Mother to Child Transmission (PMTCT) program that has been strengthened to cover wider area and is important in monitoring national trends in the future. This data will provide good estimates of national HIV prevalence and the trend.

This HIV and AIDS data aims to offer source for understanding the HIV epidemic in Kenya, in order to provide important insights into the impact of the HIV epidemic. This study focuses only on HIV cases among adults, that is, men and women aged 15-64 years. The data set is used in Chapter Four to illustrate and compare various disease mapping models proposed in Chapters Three. These comparison are in terms of cross-sectional and trend estimate of the HIV epidemic in Kenya. The results are then presented in the form of prevalence, incidence, relative risks and posterior probabilities.

1.7 Thesis Outline

This thesis aims at development of Bayesian hierarchical spatial and spatio-temporal disease mapping models. The thesis is structured in form of Chapters and it comprises of five chapters described below.

Chapter One serves as an introduction to the study. It gives an overview of the thesis and brief introduction to the concepts of Spatial Statistics and disease mapping. A statement of the problem and the objectives of the study are also given in this Chapter.

Chapter Two covers literature review in which statistical reviews and recent developments in spatial and spatio-temporal disease mapping are considered. First, an overview of classical disease mapping models is given. It then gives extensions of the classical disease mapping models. In particular, models with non-Gaussian random effect distributions, skew-t spatial combined random effects model and spatio-temporal models are discussed.

Chapter Three gives the methodology used in the thesis. First, this chapter extends the classical disease mapping models by introducing more flexible distributions for the spatially unstructured random effects. In particular, the skew-normal and skew-t distributions are discussed. Skew-t spatial combined random effects model for count data is presented in this chapter. This model is based on the so-called combined model and it uses a single framework to capture overdispersion, spatial correlation and the skewness in the data. Then Spatio-temporal models for disease mapping are discussed, in which linear time trend and non-parametric dynamic time trend models are explored. Various space-time interaction models are also given. Bayesian inference techniques are also discussed. In particular, the MCMC and INLA techniques are discussed. Finally, methods for Bayesian model comparison and goodness of fit (GOF) are also explored in this chapter. In particular, the effective number of parameters (pD), deviance information criterion (DIC) and the mean squared predictive error (MSPE) are discussed.

Chapter Four gives results and discussions on the applications of the proposed models to HIV and AIDS data. First, the use of the skew-normal and skew-t distributions is investigated and applied to 2016 Kenya HIV and AIDS data. The skew-distributions allows for the flexibility of random-effects distribution to adjust for the deviation from the usual normality assumption. Secondly, application of skew-t spatial combined random effects model to 2016 Kenya HIV and AIDS data is then presented. Then spatio-temporal variation of HIV in Kenya is given in which various space-time interaction models are given and fitted to the 2013-2016 Kenya HIV data set. Simulation studies to assess the performance of the proposed models are also presented in this chapter.

Chapter Five provides general conclusions of the main results and the recommendations for further research. List of references is given at the end of the thesis.

CHAPTER TWO

LITERATURE REVIEW

Disease mapping models and analysis have attracted tremendous growth in the recent past both in the methodological and applications aspects. This chapter reviews the literature about Bayesian hierarchical disease mapping models. First, it gives an overview of the Bayesian hierarchical disease mapping models. Secondly, it discusses non-Gaussian random effects distributions in disease mapping. It then discusses the skew-t spatial combined random effects model and spatio-temporal models for disease mapping.

2.1 Bayesian Hierarchical Disease Mapping Models

Over the past decades and with the advent of computational methods and statistical methodology, and availability of spatially-referenced data and fast software tools, disease mapping has increased in popularity in epidemiological research (Lawson and Lee, 2017; Ugarte *et al.*, 2017; Riebler *et al.*, 2016; Elliott and Wartenberg, 2004).

Suppose the study region is divided into n areas labeled $i = 1, 2, ..., n$. Let Y_i be the observed count of disease in the ith area, E_i denote the expected count in the ith area and ω_i be the unknown relative risk in that area. Here the expected counts are assumed to be known constants. The standardized incidence ratio (SIR) is usually the basic technique use to estimate the relative risk of a disease for a given area i (Neyens *et al.*, 2012). SIR is defined as the ratio of observed counts to the expected counts: $\widehat{\omega}_i = \text{SIR}_i = \frac{Y_i}{E_i}$. If $\widehat{\omega}_i = \text{SIR}_i > 1$ in a given area, then the risk of the disease is higher than expected for that region while $\widehat{\omega}_i < 1$ will imply a lower risk of the disease than expected for that area. However for the case of a rare disease and very low populated areas, the expected counts E_i can be very low which may results in unnecessarily high risk of the disease for that respective areas. Another assumption is that the areas under study are independent, which is often not practically realistic in most epidemiological studies. Therefore the use of SIR estimates do not capture the extra variability or spatial correlation due to unobserved heterogeneity present in the data (Neyens *et al.*, 2012).

To overcome this problem, Bayesian hierarchical spatial models can be used so that the joint posterior distribution for process and parameters given data can be obtained (Coly *et al.*, 2019). Such models allow the use of covariates that can provide information on the risk of mortality, as well as a set of random effects that capture the dependence between neighbouring regions (Lawson and Lee, 2017). Bayesian estimation procedure has several potential advantages as compared to the classical (e.g. maximum likelihood) estimation procedures. First, Bayesian inference allows us to express uncertainty about model parameters through prior distributions. Secondly, the availability of advanced softwares for Bayesian analysis such as WinBUGS (Spiegelhalter *et al.*, 2002) for MCMC algorithm and `R-INLA` (Martino and Rue, 2009) for INLA technique provide a flexible way to model complex disease mapping models.

Disease mapping models basically extends from the generalized linear models (GLM). Suppose Y_i are the counts of disease cases observed for a set of regions $i = 1, ..., n$ partitioning a study domain $\mathcal{D}$. The counts are normally modeled as either Poisson or Binomial random variables in the GLM framework, using a log or logit link function, respectively (Coly *et al.*, 2019; Kassahun *et al.*, 2012; Molenberghs *et al.*, 2010; Agresti, 2002). For modeling rare diseases, the appropriate model to use is the Poisson model. When the values of region-specific fixed covariates $\boldsymbol{x}_i$ with associated parameters $\boldsymbol{\beta}$ are observed, these can be included in the model in the GLM manner.

Overdispersion or spatial correlation due to unobserved heterogeneity present in count data is usually not captured by simple covariate models and it is often appropriate to include some additional term or terms in a model in order to capture such effects. Basically, overdispersion or extra-variation can be accommodated by either inclusion of a prior distribution for the relative risk (such as a Poisson-gamma model) or by extension of the linear or non-linear predictor term to include an extra random effect (log-normal model). The later leads to a hierarchical generalized linear mixed model (GLMM) with one set of random effects (Lawson and Lee, 2017; Riebler *et al.*, 2016), often modeled with Gaussian exchangeable prior distributions. In Bayesian setting, the model is specified in a hierarchical structure which allows the overall distribution of Y_i to be defined in two stages. At the first stage, observations Y_i are conditionally independent given the values of the random affects. The second stage specify the distribution of the random effects thus allowing a mechanism for inducing extra-Poisson variability in the marginal distribution of the $Y_i^{'}$s.

Correlated random effects can be introduced using a spatial covariance matrix. This can be achieved by considering the random effects to form a single vector following an appropriate distribution with a specified mean and a spatial variance-covariance matrix. There are two approaches of defining spatially structured prior formulation of the random effects. The most popular is the multivariate Gaussian distribution (Waller and Gotway, 2004; Gaetan and Guyon, 2010; Sherman, 2011). The spatial variance-covariance matrix is made up of parametric functions defining the covariance structure based on location of any two units of study. In the case of areal data, the neighbourhood structure can be specified based on the basis of sharing a border, the distance between the centroids of any pair of regions or a combination of these two (Waller and Gotway, 2004; Cressie, 1993).

Clayton and Kaldor (1987) modified the hierarchical structure by replacing the set of exchangeable priors at the second stage with a spatially structured prior distribution, leading to local empirical Bayes estimates obtained as a weighted average of observations of neighboring regions thus borrowing strength locally rather than globally. As an alternative to multivariate Gaussian models, Besag *et al.* (1991) extended the approach to a fully Bayesian setting using the MCMC algorithm. Their model is called conditional autoregressive (CAR) model.

In the CAR formulation, conditional distribution of a random effect in a region given all the other random effects is simply the weighted average of all the other random effects. Besag *et al.* (1991) assigned the weights based on whether a pair of regions shared a boundary or not; if the regions share a boundary, the weight is 1, otherwise it is 0. Other weighting possibilities include Leroux *et al.* (1999), MacNab and Dean (2000) and Green and Richardson (2002). The CAR formulation has computational advantage over the multivariate Gaussian distribution in the sense that the variance component in multivariate Gaussian requires matrix inversion at each update when executing the algorithm during estimation, leading to more computational burden which is not the case in CAR.

Up to this far, models borrowing strength either globally or locally have been discussed. Besag *et al.* (1991) suggested the inclusion of both spatially structured and spatially unstructured random effects in the same model through a convolution prior so that the model allows borrowing of information both locally and globally. Therefore they proposed the popular Besag-York-Molli´e model (BYM) model in which the unstructured random effect assumes a Gaussian exchangeable prior while the spatially structured random effect assumes an intrinsic conditional autoregressive (ICAR) prior.

There is an extensive literature in Bayesian hierarchical disease mapping models that have been used to estimate disease relative risks. In these models, covariates and a set of random effects can be included so as to respectively provide more information on the incidence risk and account for the correlation between the neighbouring ares. The following subsections outline the classical Bayesian hierarchical disease mapping models.

2.1.1 Poisson-gamma Model

A Poisson-gamma (PG) model is a mixed model obtained by allowing the Poisson mean to have a gamma distribution. It is defined as (Lawson and Lee, 2017):

$$\begin{aligned} Y_i &\sim \text{Poisson}(E_i \omega_i); \\ \omega_i &\sim \text{Gamma}(a, b) \end{aligned} \tag{2.1}$$

where Y_i and E_i denote, respectively, the observed and expected cases of disease in the ith area ($i = 1, ..., n$); ω_i is the the relative risk and the parameters a, b are assumed to be fixed and known. Here, the mean and variance of the relative risk are given by $E(\omega)_i = a/b$ and $Var(\omega_i) = a/b^2$ (Lawson and Lee, 2017).

The Poisson-gamma model has been one of the popular models in disease mapping due to its conjugacy feature that make it possible to obtain a closed form posterior distribution (Neyens *et al.*, 2012). However, this model only captures overdispersion or uncorrelated heterogeneity (UH) but does not takes into account the spatial correlation or correlated heterogeneity (CH) in the data. Additionally, this model does not provide for the inclusion of covariate effects.

2.1.2 Poisson-lognormal Model

Poisson-lognormal model assumes that the relative risk ω_i is directly linked to a linear predictor $\eta_i = \boldsymbol{x}_i^{'}\boldsymbol{\beta} + v_i$ where v_i denotes the unobserved random effects and $\boldsymbol{x}_i$ are the optional covariates. For the simplest case where there is only uncorrelated heterogeneity and no covariates, $\eta_i = v_i$. This model falls in the class of generalized linear mixed models (GLMMs) and is generally given by (Lawson and Lee, 2017);

$$\begin{aligned} Y_i &\sim \text{Poisson}(E_i\omega_i); \\ \omega_i &= \exp(\beta_0 + \boldsymbol{x}_i^{'}\boldsymbol{\beta} + v_i); \\ v_i &\sim N(0, \sigma_v^2) \end{aligned} \tag{2.2}$$

where β_0 is the global intercept peculiar to all regions and $\boldsymbol{\beta}$ is a vector of fixed effect regression coefficients corresponding the vector of covariates $\boldsymbol{x}_i$. In this case the uncorrelated heterogeneity (UH) due to the extra-variation is modeled with a zero mean Gaussian prior distribution.

The PG and PLN models behave in a similar manner in some aspects. However, the mean-variance relationship of the random-effect terms differs because it is linear in the gamma distribution and is quadratic in the lognormal distribution thus causing difference in estimating UH (Neyens *et al.*, 2012; Kim *et al.*, 2002). PLN model has become more popular than the PG model in disease mapping since the covariates can be easily included and the straightforward Bayesian inference which is implemented in advanced softwares such as WinBUGS (Spiegelhalter *et al.*, 2007). Although this model only account for the extra-variation due to overdispersion, it can be easily extended to capture spatial correlation by introducing a CH parameter resulting in a convolution model.

2.1.3 Spatial Gaussian Conditional Autoregressive Models

In the disease mapping paradigm, Gaussian conditional autoregressive (CAR) priors (Besag *et al.*, 1991; Cressie, 1993; Leroux *et al.*, 1999) are often used to model spatial correlation. For modeling areal count data, the exchangeable random effects v_i in the Poisson-lognormal model is often replaced by a spatially correlated random effects u_i

to obtain a spatial random effects model below.

$$\begin{aligned} Y_i &\sim \text{Poisson}(E_i\omega_i), \\ \omega_i &= \exp(\beta_0 + \boldsymbol{x}_i^{'}\boldsymbol{\beta} + u_i \end{aligned} \tag{2.3}$$

The joint distribution of the random effects $\boldsymbol{u} = (u_1, ..., u_n)$ often has a multivariate normal distribution (Rampaso *et al.*, 2016):

$$\boldsymbol{u} \sim \text{MVN}\left(\mu, \boldsymbol{\Sigma}\right) \tag{2.4}$$

where μ is the mean vector and $\boldsymbol{\Sigma} = \sigma_u^2\boldsymbol{\Phi}$ is the variance covariance matrix which determines the spatial structure; σ_u^2 is the variance parameter and $\boldsymbol{\Phi}$ is the precision matrix given by $\boldsymbol{\Phi} = (\boldsymbol{I} - \rho\boldsymbol{W})^{-1}\boldsymbol{M}$, where $\boldsymbol{I}$ is a $n \times n$ identity matrix, ρ is a parameter that measures spatial correlation; $\boldsymbol{W}$ is a non-negative symmetric $n \times n$ spatial proximity or weight matrix with zero elements on its diagonal, that is $w_{ii} = 0$ and $w_{ij} = 1$ if the ith and jth areas are neighbours ($i \sim j$) and 0 otherwise; $\boldsymbol{M}$ is a diagonal matrix, that is $\boldsymbol{M} = M_{ii} = diag(n_i)$, where n_i is the number of neighbours of the ith area.

The precision matrix $\boldsymbol{\Phi}$ can be specified in various ways to give rise to different CAR prior models.

2.1.4 Intrinsic Conditional Autoregressive Model

The Intrinsic conditional autoregressive (ICAR) model was proposed by Besag *et al.* (1991) and is obtained by allowing the joint distribution of the random effects $\boldsymbol{u}$ to have a multivariate normal distribution with mean vector $\mathbf{0}$ and variance matrix $\sigma_u^2\boldsymbol{Q}^-$ (where $\boldsymbol{Q}^-$ is the generalized inverse of $\boldsymbol{Q}$), with the ijth element of matrix $\boldsymbol{Q}$ defined by;

$$q_{ij} = \begin{cases} n_i, \text{ if } i = j \\ -1, \text{ if } i \sim j \\ 0, \text{Otherwise} \end{cases} \tag{2.5}$$

:

The univariate full conditional distribution of u_i given all the remaining components $\boldsymbol{u}_{-i} = (u_1, ..., u_{i-1}, u_{i+1}, ..., u_n)$ is given by (Rampaso *et al.*, 2016);

$$u_i \mid \boldsymbol{u}_{-i}, \sigma_u^2 \sim \text{Normal}\left(\frac{1}{n_i}\sum_{i\sim j}^{n} u_j, \frac{\sigma_u^2}{n_i}\right) \tag{2.6}$$

The ICAR model, however, is improper and it treats the strength of spatial correlation between random effects as maximum $(\rho = 1)$ (MacNab, 2011; Botella-Rocamora *et al.*, 2013).

2.1.5 Proper Conditional Autoregressive model

Cressie (1993) proposed the proper conditional autoregressive (named pCAR hereafter) as an alternative approach for modeling different levels of spatial correlation. He used a single set of random effects, but introduced a spatial smoothing parameter ρ that measures spatial correlation by allowing the random effects $\boldsymbol{u} = (u_1, ..., u_n)$ to have a multivariate normal distribution with precision matrix $\Phi = \boldsymbol{D^{-1}}$, that is,

$$\boldsymbol{u} \sim \text{MVN}\left(\mu, \sigma_u^2 \boldsymbol{D^{-1}}\right) \tag{2.7}$$

so that the ijth element of matrix $\boldsymbol{D}$ defined by;

$$d_{ij} = \begin{cases} n_i, \text{ if } i = j \\ -\rho, \text{ if } i \sim j \\ 0, \text{Otherwise} \end{cases} \tag{2.8}$$

If $0 \leq \rho < 1$,then the joint distribution of $\boldsymbol{u}$ in (2.7) is proper (Rampaso *et al.*, 2016). The univariate full conditional distribution for the random effects u_i is given by (Lee, 2011):

$$u_i \mid \boldsymbol{u}_{-i}, \sigma_u^2, \rho \sim \text{Normal}\left(\frac{\rho}{n_i}\sum_{i\sim j}^{n} u_j, \frac{\sigma_u^2}{n_i}\right) \tag{2.9}$$

Taking $\rho = 0$ implies there is no spatial dependence and values of ρ closer to one indicate strong spatial dependence in the data ($\rho = 1$ reduces to the ICAR model).

Rampaso *et al.* (2016) noted that for ρ close to zero, i.e when there is absence of spatial dependence between the random effects, this model has a weakness in that the conditional variance does not change and it continue to depend on the number of neighbours n_i.

2.1.6 Leroux Conditional Autoregressive Model

As an alternative to the ICAR and pCAR models, Leroux *et al.* (1999) proposed a more general conditional autoregressive model (named LCAR hereafter) in which the precision matrix is given by $\boldsymbol{\Phi} = \rho\boldsymbol{Q} + (1-\rho)\boldsymbol{I}$, where $\boldsymbol{I}$ is a $n \times n$ identity matrix and the matrix $\boldsymbol{Q}$ is the same as defined in (2.5). It can be seen that for $\rho = 0$, LCAR model reduces to a model with independent (exchangeable) random effects. As in the pCAR mpodel, it reduces to the ICAR model when $\rho = 1$. If $0 \leq \rho < 1$, then the joint distribution of $\boldsymbol{u}$ with precision matrix $\boldsymbol{\Phi} = \rho\boldsymbol{Q} + (1-\rho)\boldsymbol{I}$ is proper (Rampaso *et al.*, 2016).

The univariate full conditional distribution is then given by (Lee, 2011);

$$u_i \mid \boldsymbol{u}_{-i}, \sigma_u^2, \rho \sim \text{Normal}\left(\frac{\rho}{(1-\rho)+n_i\rho}\sum_{i\sim j}^{n} u_j, \frac{\sigma^2}{(1-\rho)+n_i\rho}\right) \tag{2.10}$$

2.1.7 Convolution Model

To model the random effects, Besag *et al.* (1991) also proposed another popular model known as the convolution model (named BYM hereafter) which includes two sets of random effects in the same model: a spatially unstructured component to account for pure overdispersion and a spatially structured component to account for spatial correlation:

$$\begin{aligned} Y_i &\sim \text{Poisson}(E_i\omega_i), \\ \omega_i &= \exp(\beta_0 + \boldsymbol{x}_i^{'}\boldsymbol{\beta} + u_i + v_i), \\ u_i &\sim ICAR(\sigma_u^2);\, v_i \sim N(0, \sigma_v^2) \end{aligned} \tag{2.11}$$

The BYM model is, however, improper and has identifiability problems (Eberly and Carlin, 2000; MacNab, 2014; Rampaso *et al.*, 2016). That is, each data point is represented by two random effects but only their sum $u_i + v_i$ is only identifiable. In addition, the Gaussian exchangeable prior in this model does not capture the extra variability that may arise due to overdispersion.

2.2 Skew-Random Effect Distributions in Disease Mapping

The disease mapping models considered that have so far been considered have random effects assuming either a Gaussian (normal) exchangeable prior for the spatially unstructured heterogeneity or the popular Gaussian CAR priors for the spatially structured variability. However, this Gaussian assumption may be too restrictive because some random effects can be skewed violating this general normality assumption (Nathoo and Ghosh, 2012; Branco and Dey, 2001; Box and Tiao, 1973). Several authors (Ngesa *et al.*, 2014; Nathoo and Ghosh, 2012; Wakefield, 2007; Chen *et al.*, 2002; Best *et al.*, 1999; Besag *et al.*, 1991) have suggested that it is possible to replace this normality assumption with other choices such as the Laplace distribution, the Student t-distribution or semi non-parametric (SNP) densities. For instance, Ngesa *et al.* (2014) used generalized Gaussian distribution (GGD). Through a simulation, they found that GGD performs better than the normal distribution. Thus there is a need to consider models with more flexible non-Gaussian random effect distributions. This flexibility could arise when the random effects distribution is highly skewed or has excess kurtosis. This thesis explores the use of skew-normal (SN) and skew-t (ST) distributions as candidates for the spatially unstructured random effects. The SN and ST distributions fall in the general asymmetric class of skew-elliptical distributions (Branco and Dey, 2001) which are often used to capture skewness and excess kurtosis in the data. There is a rich literature on parametric modeling with skew-elliptical distributions. For regression analysis using the multivariate skew-t distribution, see for example Branco and Dey (2001), Sahu *et al.* (2003), and Azzalini and Capitanio (2003). To analyze spatially correlated non Gaussian data, Kim and Mallick (2004) developed skew-normal spatial Kriging process. In the context of non-Gaussian geostatistical data, Palacios (2006) proposed a formulation using scale mixing of a stationary Gaussian process.

2.3 Skew-t Spatial Combined Random Effects Model

Overdispersed count data that is spatially correlated and also possibly skewed is a common phenomenon in many practical situations. The classical random-effects models used for count data includes the Poisson-gamma model, that has a closed form posterior distribution due to the conjugate feature between the Poisson and Gamma distributions but accounts only for overdispersion or extra variation, and the Gaussian conditional autoregressive (CAR) models, such as the intrinsic CAR model (Besag *et al.*, 1991), that model spatial correlation but does not have a closed-form posterior distribution.

The popular convolution model (Besag *et al.*, 1991) has been used to model both correlated heterogeneity (CH) and uncorrelated heterogeneity (UH) in the data. This model has been widely used in disease mapping studies because of its potential to incorporate numerous weighting schemes (Neyens *et al.*, 2012) and its implementation in most Bayesian softwares such as WinBUGS (Spiegelhalter *et al.*, 2007). However, this model lacks the important conjugate feature offered by the Poisson-gamma model. There are limited studies on count data models that utilize this conjugacy. Wolpert and Ickstadt (1998) attempted to explore it by using correlated gamma field models. However, (Best *et al.*, 2005) noted poor performance of these models in simulation study to compare various disease mapping models.

Neyens *et al.* (2012) proposed a model that combines a Poisson-gamma model with normal random effects, thus accounting for both overdispersion and spatial correlation. There are limited studies extending the Poisson-gamma model to accommodate spatial correlation because of a number of reasons. First, a gamma distribution does not easily provide for extensions into covariate modeling, and, second, gamma distribution does not take into account spatial correlation or correlated heterogeneity (CH). The combined model provides a flexible way for introducing both the random effects and covariate effects.

In the Neyens *et al.* (2012) spatial combined random effects model, spatial smoothing is accomplished using a latent Gaussian Markov random field (MRF). This Gaussian assumption is, however, too restrictive in practice to capture variability which can be a problem in cases where there is high skewness and excess kurtosis. This thesis considered an alternative model that combines a Poisson-gamma model with a spatially structured skew-t random effect in the same model thus accounting for the extra variability, spatial correlation and skewness in the data.

2.4 Spatio-temporal Models for Disease Mapping

Investigating only the spatial pattern of diseases or exposures as introduced above does not allow us to say anything about their temporal variation which could be equally important and interesting. Modern registers nowadays provide a lot of information with high quality data recorded for different regions over a period of time (i.e days, months or years). This has brought in new challenges and goals which also require new and more flexible statistical models, faster and less computationally demanding methods for model fitting, and advance softwares to implement them. The spatial models introduced above can be easily extended to model temporal variation by including a time component so that the data are now defined by a process indexed by space and time. Spatio-temporal disease mapping models are often used in disease surveillance studies (Abellan *et al.*, 2008; Lawson *et al.*, 2009) where the objective is to identify the spatial patterns and the temporal variation of disease risks or rates.

Spatio-temporal models are mainly used in disease mapping studies because they provide a platform that enables borrowing of information from spatial and temporal neighbours to reduce the high variability that is common to classical risk estimators, such as the standardized mortality ratio (SMR) when the area of study has a low population or the disease under consideration is rare. These models are usually formulated in a hierarchical Bayesian framework and typically relies on generalized linear mixed models (GLMM). Model fitting and statistical inference is commonly accomplished through the empirical Bayes (EB) and fully Bayes (FB) approaches. The EB approach usually relies on the penalized quasi-likelihood (PQL) (Breslow and Clayton, 1993), while the FB approach usually uses Markov chain Monte Carlo (MCMC) techniques (Gilks *et al.*, 2005).

The FB approach has become more popular in disease mapping studies due to the availability of advance Bayesian softwares such as WinBUGS Spiegelhalter *et al.* (2002) for implementation of the MCMC procedure. However, there are many challenges in using the MCMC for Bayesian analysis. This includes the need to evaluate convergence of posterior samples which often consumes a lot of time due to the extensive simulation. In addition, the MCMC methods may lead to large Monte Carlo errors if the data at hand is huge and the models involved are complex or complicated as in the case of spatio-temporal models (Schrödle *et al.*, 2011). Further more, reliable inference may not be obtained if the priors of the hyperparameters are not chosen correctly (Wakefield, 2007; Fong *et al.*, 2010).

As an alternative to the MCMC, this study considered a new strategy called integrated nested Laplace Approximation (INLA) which has been recently developed (Rue *et al.*, 2009) for Bayesian inference. INLA allows fairly complex models to be fit much faster than the MCMC and is now becoming very popular in disease mapping. In addition, INLA also has a package `R-INLA` (Martino and Rue, 2009) that can be implemented easily in the free software `R` (R Core Team, 2016).

There is an extensive literature in Bayesian spatio-temporal disease mapping spanning parametric and non-parametric time trends models as well as interactions. For example, see Bernardinelli *et al.* (1995); Assunção *et al.* (2001) and Ugarte *et al.* (2009a) for parametric models and Knorr-Held and Besag (1998) for non-parametric time trends models. A major contribution to spatio-temporal disease mapping is the research paper by Knorr-Held (2000), which describes four different types of space-time interactions. Most studies in spatio-temporal disease mapping model both the spatial and temporal effects using conditional autoregressive (CAR) priors, extending the BYM (Besag *et al.*, 1991) model. Recently, other approaches that includes the use of splines have been proposed. For example, from an EB framework MacNab and Dean (2001) considered autoregressive local smoothing in space and B-spline smoothing for time. Ugarte *et al.* (2010) and Ugarte *et al.* (2012b) proposed a pure interaction P-spline model for space and time, and Ugarte *et al.* (2012a) used an Analysis of Variance (ANOVA) type P-spline model to study spatio-temporal variations of prostate cancer mortality in Spain. Within a FB framework, spline smoothing has also been considered for disease mapping models, see for example MacNab and Gustafson (2007) and MacNab (2007).

In this thesis, space-time disease mapping models were considered and fitted using the INLA methodology. Most spatial and spatio-temporal disease mapping models that have been implemented with INLA use the popular BYM convolution model (Besag *et al.*, 1991) in which the spatially structured random effect assumes an intrinsic conditional autoregressive (ICAR) prior (Held *et al.*, 2010; Schrödle *et al.*, 2011; Schrödle and Held, 2011a,b; Blangiardo *et al.*, 2013). The ICAR prior is, however, improper (MacNab, 2011; Botella-Rocamora *et al.*, 2013) and the spatial and non-spatial random effects in the BYM convolution model are not identifiable from the data (MacNab, 2014; Rampaso *et al.*, 2016). In this thesis, the Leroux conditional autoregressive (LCAR) prior proposed by Leroux *et al.* (1999) was used to model the spatially structured random effect in the spatial-temporal models considered. This prior has been shown to perform better than the ICAR prior (Lee, 2011) and can be easily implemented with the `R-INLA` package.

CHAPTER THREE

RESEARCH METHODOLOGY

This chapter discusses the methodology used in the thesis. It first discusses the proposed models, particularly, skew-random effects distributions models, skew-t spatial combined random Effects model and spatio-temporal models in Disease Mapping context. It then gives Bayesian inference techniques and methods of model comparison. Spatial and spatio-temporal models considered in this thesis were analyzed using Markov chain Monte Carlo (MCMC) and the Integrated Nested Laplace Approximation (INLA) techniques and implemented with WinBUGS and `R-INLA` Bayesian softwares respectively.

3.1 Skew-Random Effect Distributions in Disease Mapping

This section discusses the skew-normal (SN) and skew-t (ST) distributions that can be used to model the unstructured random effects.

3.1.1 Skew-normal Distribution

Definition 3.1: *A continuous univariate random variable X is said to have a skew-normal distribution with location $\mu \in \mathbb{R}$, scale $\sigma > 0$, and shape $\alpha \in \mathbb{R}$, denoted as $X \sim SN(\mu, \sigma^2, \alpha)$, if its density function is given by (Genton, 2004);*

$$p(x \mid \mu, \sigma, \alpha) = \frac{2}{\sigma}\phi\left(\frac{x-\mu}{\sigma}\right)\Phi\left(\frac{\alpha(x-\mu)}{\sigma}\right), x \in \mathbb{R} \tag{3.1}$$

where $\phi(.)$ and $\Phi(.)$ denote, respectively, the density and cumulative distribution function of the standard normal distribution. The shape parameter α determines the asymmetry of the distribution, with $\alpha > 0$ and $\alpha < 0$ corresponding, respectively, to positive and negative skewness.

Property 3.1: If $\alpha = 0$, the SN distribution reduces to the Normal distribution $N(\mu, \sigma^2)$.

Property 3.2: As $\alpha \to \infty$, SN distribution tends to the half normal distribution $N^+(\mu, \sigma^2)$, where N^+ denotes the folded (positive part) normal distribution.

Property 3.3: If $Y \sim SN(\mu, \sigma^2, \alpha)$, then $Y^2 \sim \chi^2_{(1)}$.

Property 3.4: The mean and variance of $Y \sim SN(\mu, \sigma^2, \alpha)$, are given by (Genton, 2004):

$$\begin{aligned} E(Y) &= \mu + \left(\tfrac{2}{\pi}\right)^{\frac{1}{2}} \alpha \\ Var(Y) &= \sigma^2 + \left(1 - \tfrac{2}{\pi}\right) \alpha^2 \end{aligned} \tag{3.2}$$

3.1.2 Skew-t Distribution

Let $Z \sim SN(0, \sigma^2, \alpha)$ and $X \sim \chi_v^2; v > 0$ be independent independent random variables. Then $Y = \mu + \frac{Z}{\sqrt{X/v}}$ is said to have a skew-t distribution with location μ, scale σ, shape α and v degrees of freedom, denoted as $Y \sim ST(\mu, \sigma^2, \alpha, v)$. The density function of a skew-t random variable Y is given by (Nathoo and Ghosh, 2012):

$$p(y \mid \mu, \sigma, \alpha, v) = 2t(y; \mu, \sigma, v) T \left\{ \frac{\alpha(y-\mu)}{\sigma} \left(\frac{v+1}{\frac{(y-\mu)^2}{\sigma^2} + v} \right)^{1/2} ; v+1 \right\} \tag{3.3}$$

where

$$t(y; \mu, \sigma, v) = \frac{1}{\sigma\sqrt{\pi v}} \frac{\Gamma\left\{(v+1)/2\right\}}{\Gamma(v/2)} \frac{1}{\left[1 + \frac{(y-\mu)^2}{v\sigma^2}\right]^{(v+1)/2}}, -\infty \leq y \leq \infty$$

That is, $t(y; \mu, \sigma, v)$ is the density of a student $t-$ distribution with location μ, scale σ and v degrees of freedom and $T(.; v+1)$ is the cumulative distribution function of a standard t distribution on $(v+1)$ degrees of freedom. The skew-t distribution contains the following distributions as its special cases: normal ($\alpha = 0, v \to \infty$), skew-normal ($v \to \infty$) and student-t ($\alpha = 0$).

The mean and variance of $Y \sim ST(\mu, \sigma^2, \alpha, v)$, when they exist, are given by (Azzalini and Capitanio, 2003):

$$E\left[Y \mid \mu, \sigma, \alpha v\right] = \mu + \frac{\sigma\alpha}{\sqrt{1+\alpha^2}} \left(\frac{v}{\pi}\right)^{1/2} \frac{\Gamma\left\{(v-1)/2\right\}}{\Gamma(v/2)}, v > 1 \tag{3.4}$$

$$Var\left[Y \mid \mu, \sigma, \alpha v\right] = \sigma^2 \left(\frac{v}{v-2} - \frac{\alpha^2}{1+\alpha^2} \frac{v}{\pi} \frac{\Gamma^2\left\{(v-1)/2\right\}}{\Gamma^2(v/2)} \right), v > 2 \tag{3.5}$$

In order to assess the performance of the proposed models, the following following models were fitted to the Kenya 2016 HIV and AIDS incidence data.

$$Y_i \sim \text{Poisson}(\mu_i) \tag{3.6}$$

with

1. **PLN**: $\log(\mu_i) = \log(E_i) + \beta_0 + v_i; v_i \sim N(0, \sigma_v^2)$
2. **PLSN**: $\log(\mu_i) = \log(E_i) + \beta_0 + \phi_i;\;\; \phi_i = \delta Z_i + v_i;\;\; Z_i \sim N^+(0; \sigma_z^2);$ $\delta \sim N(0, \sigma_\delta^2);\; v_i \sim N(0, \sigma_v^2)$
3. **PLT**: $\log(\mu_i) = \log(E_i) + \beta_0 + \phi_i;\;\; \phi_i = \eta_i^{-\frac{1}{2}}(v_i);\;\; \eta_i \sim \text{Gamma}(\frac{v}{2}, \frac{v}{2});$ $v_i \sim N(0, \sigma_v^2)$
4. **PLST**: $\log(\mu_i) = \log(E_i) + \beta_0 + \phi_i;\;\; \phi_i = \eta_i^{-\frac{1}{2}}(\delta Z_i + v_i);\;\; Z_i \sim N(0; \sigma_z^2);$ $\delta \sim N(0, \sigma_\delta^2);\; v_i \sim N(0, \sigma_v^2)$

where Y_i and E_i denote, respectively, the observed and expected cases of HIV and AIDS in the ith county ($i = 1, ..., 47$); δ is the skewness parameter; $\boldsymbol{Z}$ are skewing variables and k is the number of degrees of freedom for the t distribution.

3.2 Skew-t Spatial Combined Random Effects Model for Areal Count Data

This section discusses the skew-t spatial combined random effects model that can be used in to account for the extra variability, spatial correlation and skewness in the data.

Let $\boldsymbol{u}, \boldsymbol{Z}, \boldsymbol{\eta} \in \mathbb{R}^n$ be mutually independent random vectors and define $\delta \in \mathbb{R}$ so that the region-specific random effects $\boldsymbol{S} = (s_1, \ldots, s_n)'$ are defined by

$$S_i = \eta_i^{-\frac{1}{2}}(\delta Z_i + u_i) \tag{3.7}$$

where u_i are spatially structured random effects for modeling correlated heterogeneity (CH) and was assumed to follow a proper CAR prior (2.7), that is $\boldsymbol{u} \sim \text{MVN}\left(\mu, \sigma_u^2 \boldsymbol{D^{-1}}\right)$ with d_{ij} equal to n_i if $i = j$, -1 if $i \sim j$ and 0 otherwise, where $n_{i,}$ is the number of neighbours of county i and $i \sim j$ indicates that counties i and j are neighbours; δ is the skewness parameter; $\boldsymbol{Z}$ are skewing variables each following identically independent standard normal distribution $Z_i \sim N(0,1)$; $\boldsymbol{\eta}$ is a scale mixing parameter with $\eta_i \sim \text{Gamma}(k/2, k/2)$.

In a similar version to the spatial combined model of Neyens *et al.* (2012), the proposed model is now defined as follows:

$$
\begin{aligned}
Y_i &\sim \text{Poisson}(\mu_i = E_i\omega_i) \\
\omega_i &= \theta_i h_i;\ h_i = \exp(\beta_0 + \boldsymbol{x}_i'\boldsymbol{\beta} + S_i) \\
\log(\mu_i) &= \log(E_i) + \log(\theta_i) + \boldsymbol{x}_i'\boldsymbol{\beta} + S_i \\
S_i &= \eta_i^{-\frac{1}{2}}(\delta Z_i + u_i); Z_i \sim N(0,1); u_i \sim \text{pCAR}(\sigma_u^2); \\
\eta_i &\sim \text{Gamma}(k/2, k/2); \delta \sim \text{N}(0, \sigma_\delta^2); \theta_i \sim \text{Gamma}(a, b)
\end{aligned}
\tag{3.8}
$$

where E_i is the expected number of counts for region i and ω_i is the unknown relative risk in that region; β_0 is the global intercept common to all regions and $\boldsymbol{\beta}$ is a vector of fixed effect regression coefficients corresponding the vector of covariates $\boldsymbol{x}_i$; θ_i is the overdispersion random effects parameter for modeling uncorrelated heterogeneity(UH) and was assumed to follow a gamma distribution.

The above model combines a Poisson-gamma model with a spatially structured skew-t random effects in the same model thus accounting for the extra variability, spatial correlation and possible skewness in the data.

The marginal distribution of each spatial effect S_i falls in the skew-t family of distributions (MacNab, 2003; Nathoo and Ghosh, 2012). In particular, we have that $S_i \mid \sigma_u, \rho, \delta, v \sim ST(\mu_i, \sigma_i, \alpha_i, k_i)$ with location $\mu_i = 0$, scale $\sigma_i = \sqrt{\delta^2 + \Sigma_{ii}}$, shape $\alpha_i = \frac{\delta}{\Sigma_{ii}}$ and degrees of freedom $k_i = k$. As in the case of standard Gaussian pCAR (ρ, σ_u^2) model, the parameter ρ represents the spatial smoothing parameter.

As in the Poisson-gamma model, a closed-form posterior distribution can be obtained because of the strong conjugacy between the Poisson and gamma distributions. That is;

$$
\begin{gathered}
\pi(\boldsymbol{\omega} \mid \boldsymbol{Y}) \propto p(\boldsymbol{Y} \mid \boldsymbol{\omega}) \times p(\boldsymbol{\omega}) \\
\pi(\omega_i \mid Y_i) \propto (e^{-E_i h_i \theta_i}\theta_i^{Y_i}) \times (\theta_i^{a-1}e^{-b\theta_i}) \\
\Longrightarrow \pi(\omega_i \mid Y_i) \propto \theta_i^{a+Y_i-1}e^{-(b+E_i h_i)\theta_i} \\
\text{where } h_i = \exp(\beta_0 + \boldsymbol{x}_i'\boldsymbol{\beta} + S_i)
\end{gathered}
$$

$$\therefore\ \omega_i \mid Y_i \sim \text{Gamma}(a^*, b^*)$$
$$\text{where } a^* = a + Y_i \text{ and } b^* = b + E_i h_i \tag{3.9}$$

Thus, the conditional mean of ω_i given the random effects S_i is $(a + Y_i)/(b + E_i h_i)$, and can be re-written as a weighted average of the prior mean a/b and the area-specific standardized incidence rate Y_i/E_i, with weights $b/(b + E_i h_i)$ and $E_i/(b + E_i h_i)$, respectively. It can also be re-written as a weighted average of the prior mean a/b and the ratio of the incidence rate versus spatially-structured relative risk $(Y_i/E_i)/g_i$, with weights $1 - w_i$ and w_i, respectively, with $g_i = E_i h_i/(b + E_i h_i)$. While these full conditionals are not of primary interest, this relationship can give us an understanding of how smoothing is obtained in this model. The weights w_i are inversely related to the variance of Y_i/E_i. Thus, for rare diseases and small areas, there is a lot of shrinkage to the prior mean a/b. This is similar to the Poisson-gamma model. When a large amount of overdispersion is present in the data (b small), there will be less shrinkage to the prior mean a/b. Note that the weights g_i depend on the spatial smoothing parameter ρ. If ρ contains a strongly spatially-structured effect, the weights (and the amount of shrinkage) will also be spatially structured.

This model is closely related to the skew-t spatial model. The only difference is that apart from the parameters δ and k that control the skewness and excess kurtosis, the proposed model has an additional gamma distributed parameter θ that accounts for overdispersion. Note that this skew-t combined model provides an amalgamation of the Poisson-gamma model on one hand and the skew-t pCAR model on the other hand, thereby taking the best features of both: the skewness parameter with and linear predictor with the CAR-term which can include covariate effects from the pCAR model on one hand (Nathoo and Ghosh, 2012) and the overdispersion term with the conjugacy characteristic from the Poisson-gamma model on the other hand (Molenberghs *et al.*, 2007).

This generalization of the Gaussian CAR model to a five-parameter model that has additional parameters δ, k and θ to control the skewness, excess kurtosis and overdispersion in the marginal distributions is referred to as $STCAR(\sigma_u, \rho, \delta, k, \theta)$. Setting $\exp(\beta_0 + \boldsymbol{x}_i'\boldsymbol{\beta} + S_i) = 1$ yields Poisson-gamma model (2.1) and letting $\theta_i = 1$ corresponds to skew-elliptical Poisson spatial model. While letting $\rho = 0$ and $\theta_i = 1$ results in uncorrelated skew-t random effects model. If $\delta = 0$ and $k \to \infty$ then the model reduces to the spatial combined model (Neyens *et al.*, 2012). If in addition $\theta_i = 1$ then it leads to the Gaussian pCAR(ρ, σ_u^2) given by (2.9). The standard BYM model is obtained by letting $\theta_i = 1$ and $S_i = u_i + v_i$ such that $v_i \sim N(0, \sigma_v^2)$ and setting $\rho = 1$ in (2.6).

The skew-t conditional autoregressive combined (STCARCOM) model proposed in this thesis was compared to the existing classical disease mapping models: Poisson-gamma (PG), Poisson-lognormal (PLN), intrinsic conditional autoregressive correlated heterogeneity (ICAR CH), convolution (CON), and the skew-t conditional autoregressive (STCAR). The following models were therefore fitted to the 2016 Kenya HIV and AIDS data.

$$Y_i \sim \text{Poisson}(\mu_i) \tag{3.10}$$

with

1. **PG**: $\log(\mu_i) = \log(E_i) + \log(\omega_i); \omega_i \sim$ Gamma(a, b)

2. **PLN**: $\log(\mu_i) = \log(E_i) + \beta_0 + v_i;\ v_i \sim N(0, \sigma_v^2)$

3. **ICAR CH**: $\log(\mu_i) = \log(E_i) + \beta_0 + u_i; u_i \sim$ ICAR(σ_u^2)

4. **CON**: $\log(\mu_i) = \log(E_i) + \beta_0 + u_i + v_i;\ u_i \sim$ ICAR(σ_u^2), $v_i \sim N(0, \sigma_v^2)$

5. **STCAR**: $\log(\mu_i) = \log(E_i) + \beta_0 + S_i; S_i = \eta_i^{-\frac{1}{2}}(\delta Z_i + u_i);$
   $Z_i \sim N(0, 1); u_i \sim$ pCAR(σ_u^2); $\eta_i \sim$ Gamma$(k/2, k/2)$

6. **STCARCOM**: $\log(\mu_i) = \log(E_i) + \log(\theta_i) + \beta_0 + S_i; S_i = \eta_i^{-\frac{1}{2}}(\delta Z_i + u_i);$
   $Z_i \sim N(0, 1); u_i \sim$ pCAR(σ_u^2); $\eta_i \sim$ Gamma$(k/2, k/2)$; $\theta_i \sim$ Gamma(a, b)

where Y_i and E_i are, respectively, the observed and expected cases of HIV and AIDS in the ith county ($i = 1, \ldots, 47$).

3.3 Spatio-temporal Models for Disease Mapping

Suppose that for every small area i, say county, HIV and AIDS data is available for different time periods $t = 1, ..., T$. Then, conditional on the relative risk θ_{it}, Y_{it} which is the number of HIV and AIDS cases in county i at time t is assumed to be Poisson distributed with mean $\mu_{it} = E_{it}\theta_{it}$, where E_{it} is the expected number of HIV and AIDS cases. That is;

$$\begin{aligned} Y_{it} \mid \theta_{it} &\sim \text{Poisson}(\mu_{it} = E_{it}\theta_{it}); \\ \log(\mu_{it}) &= \log(E_{it}) + \log(\theta_{it}) \end{aligned} \tag{3.11}$$

Here, $\log(\theta_{it})$ can be specified in different ways to define various models.

3.3.1 Parametric Linear time trend models

This subsection presents a spatio-temporal model with a parametric linear trend similar to the model proposed by Bernardinelli *et al.* (1995) for modeling the temporal component. This model extends the BYM spatial model (Besag *et al.*, 1991) by including both a linear time trend and a differential time trend for each small area, and is defined as:

$$\begin{aligned} Y_{it} \mid \theta_{it} &\sim \text{Poisson}(\mu_{it} = E_{it}\theta_{it}); \\ \log(\mu_{it}) &= \log(E_{it}) + \beta_0 + u_i + (\beta + \delta_i).t \end{aligned} \tag{3.12}$$

where β_0 is the intercept that represents the average incidence rate in the entire study area, u_i is the spatial random effect, β is the main linear time trend which measures the global time effect, and δ_i is a differential trend which quantifies the interaction between the linear time trend and the spatial effect u_i. A Leroux conditional autoregressive (LCAR) prior (2.10) proposed by Leroux *et al.* (1999) was used to model the spatial effects u_i while the intercept β_0 and the differential trend δ_i were modeled using Gaussian exchangeable prior distributions $\beta_0 \sim N(0, \sigma^2_{\beta_0})$ and $\delta_i \sim N(0, \sigma^2_{\delta})$ respectively.

3.3.2 Non-parametric dynamic time trend models

In the parametric linear trend model (3.12), a linearity assumption is imposed on the differential temporal trend δ_i. However, this assumption is usually violated in many practical situations where change points in the temporal trends are often observed due advances in research that have led to improvements in diagnosis, treatments, and early detection and intervention. As an alternative to the parametric linear trend model, this thesis considered dynamic non-parametric space-time interactions models of the form;

$$\begin{aligned} Y_{it} \mid \theta_{it} &\sim \text{Poisson}(\mu_{it} = E_{it}\theta_{it}); \\ \log(\mu_{it}) &= \log(E_{it}) + \beta_0 + u_i + \phi_t + \gamma_t + \delta_{it} \end{aligned} \tag{3.13}$$

Here β_0 and u_i have the same parametrization as in equation (3.12). ϕ_t denotes the temporally unstructured and structured random effect modeled using a Gaussian exchangeable prior with mean 0 and variance σ^2_{ϕ}. That is, $\boldsymbol{\phi} \sim N(\mathbf{0}, \sigma^2_{\phi}\boldsymbol{I}_t)$ where $\boldsymbol{I}_t$ is a $T \times T$ identity matrix. γ_t is the temporally structured random effect modeled dynamically using a random walk of order 1(RW1) or order 2 (RW2). That is, $\gamma_t \mid \gamma_{t-1} \sim N(\gamma_{t-1}, \sigma^2)$ for RW1 and $\gamma_t \mid \gamma_{t-1}, \gamma_{t-2} \sim N(2\gamma_{t-1} + \gamma_{t-2}, \sigma^2)$ for RW2; while δ_{it} represents the space–time interaction term, which was assumed to follow a Gaussian distribution with precision matrix given as $\sigma^2_{\delta}\boldsymbol{R}_{\delta}$, where σ^2_{δ} is the variance parameter and $\boldsymbol{R}_{\delta}$ is the structure matrix given by the Kronecker product of the respective structural matrices which represents the type of the temporal and/or spatial main effects which interact (Rampaso *et al.*, 2016). The additive models can be obtained by leaving out the interaction terms.

There are four ways to define the structure matrix $\boldsymbol{R}_{\delta}$ (Knorr-Held, 2000; Ugarte *et al.*, 2014) as presented in Table 3.1. This table gives a summary of the structure matrices for the different type of space-time interactions and the rank deficiencies.

Table 3.1: *Specification and rank deficiency for different space-time interactions*

		Rank of $\boldsymbol{R}_{\delta}$	
Space-time interaction	$\boldsymbol{R}_{\delta}$	***RW1*** for γ	***RW2*** for γ
Type I	$\boldsymbol{I}_s \bigotimes \boldsymbol{I}_t$	*I.T*	*I.T*
Type II	$\boldsymbol{I}_s \bigotimes \boldsymbol{R}_t$	*I.(T-1)*	*I.(T-2)*
Type III	$\boldsymbol{R}_s \bigotimes \boldsymbol{I}_t$	*(I-1).T*	*(I-1).T*
Type IV	$\boldsymbol{R}_s \bigotimes \boldsymbol{R}_t$	*(I-1)(T-1)*	*(I-1)(T-2)*

Source: Ugarte *et al.* (2014)

For Type I interactions, all δ_{it}'s are a priori independent. Therefore, it is assumed that there is no spatial and/or temporal structure on the interaction and therefore $\delta_{it} \sim N(0, 1/\tau_{\delta})$. In Type II interactions, each $\delta_{i.}, i = 1, ..., n$ follows a random walk (RW1 or RW2), independently of all other areas. Type II interactions are appropriate if the temporal trends differ from one area to another, but have no structure in space. In

Type III interactions, the parameters of the tth time point $\{\delta_{.1}, ..., \delta_{.T}\}$ have a spatial structure independent from the other time points. Hence each $\delta_{.t}$, $t = 1, ..., T$ follows an independent ICAR prior. Type III interactions can be seen as different spatial trends for every time point with no temporal structure. Type IV interaction assumes that $\delta_{it}^{\prime}$s are completely dependent over space and time. This type of interaction is the most complex among the space-time interactions, and is appropriate if the temporal trends differ from one area to another, but are more likely to be the same for neighbouring areas. To ensure that the interaction term $\boldsymbol{\delta}$ is identifiable in case of rank deficiency, sum-to-zero constraints have to be used. If these constraints are not included then the interaction terms are confounded with the main time effect $\boldsymbol{\gamma}$. It is only the Type I interaction which does not need additional constraints as this prior does not induce a rank deficiency as seen in Table 3.1.

To ensure that the interaction term $\boldsymbol{\delta}$ is identifiable, it is emphasized here that sum-to-zero constraints should be used depending on the type of interaction (see Table 3.1). The vector $\boldsymbol{\delta}$ belongs to the general class of intrinsic Gaussian Markov random field (IGMRF) which is improper, i.e. its precision matrix or equivalently its structure matrix $\boldsymbol{R}_{\delta}$ is not of full rank. Its improper distribution denoted by $\pi^*(\boldsymbol{\delta})$ is expressed as (Ugarte *et al.*, 2014; Schrödle and Held, 2011b):

$$\pi^*(\boldsymbol{\delta}) = \pi(\boldsymbol{\delta} \mid \boldsymbol{A}\boldsymbol{\delta} = \boldsymbol{e}) \tag{3.14}$$

where $\boldsymbol{A}\delta = \boldsymbol{e}$ denotes linear constraints on $\boldsymbol{\delta}$ with matrix $\boldsymbol{A}$ given by those eigenvectors of $\boldsymbol{R}_{\delta}$ which span the null space. Hence, to ensure that $\boldsymbol{\delta}$ is identifiable, the null space of the corresponding structural matrix $\boldsymbol{R}_{\delta}$ is determined using the eigenvectors obtained as linear constraints for the estimation of $\boldsymbol{\delta}$. Thus, the number of linear constraints required is always equal to the rank deficiency of $\boldsymbol{R}_{\delta}$ (see Table 3.1) and $\boldsymbol{e}$ is a vector of zeros.

3.3.3 Prior distributions

For the spatio-temporal disease mapping models considered in this thesis, the vector of parameters is given by $\boldsymbol{x} = (\beta_0, \boldsymbol{u}^{\prime}, \boldsymbol{\phi}^{\prime}, \boldsymbol{\gamma}^{\prime}, \boldsymbol{\delta}^{\prime})^{\prime}$ while the vector of hyperparameters representing the unknown variance parameters and the spatial smoothing parameter is given by $\boldsymbol{\theta} = (\sigma_s^2, \rho_s, \sigma_\phi^2, \sigma_\gamma^2, \sigma_\delta^2)'$. The choice of prior distributions for the parameters is very important in Bayesian estimation because it can seriously affect the posterior distributions. Here, $\log \tau_s$ ~logGamma$(1, 0.01)$ and logit(ρ_u)~logitbeta$(4, 2)$ were used as the hyperprior distributions for the spatial components (Ugarte *et al.*, 2014). The informative prior for ρ_u was used since the data at hand are known to show high spatial correlation . If no information about the amount of spatial correlation is available, a non informative prior such as a logitbeta(1,1) can be used (Ugarte *et al.*, 2014). For the temporally unstructured random effect $\boldsymbol{\phi}$, a $\log \tau_\phi$ ~logGamma(1,0.01) hyperprior was used (Schrödle and Held, 2011b). For the temporally structured random effect $\boldsymbol{\gamma}$, RW1 or RW2 were used while for the interaction term $\boldsymbol{\delta}$, the default priors minimally informative priors log$\tau_\gamma \sim$ logGamma$(1, 0.00005)$, log$\tau_\delta \sim$ logGamma$(1, 0.00005)$ were used. Finally, a Gaussian exchangeable prior with mean 0 and variance 0.000001 was used for the fixed effect β_0. For further details on choosing the priors for the precision parameters, see Ugarte *et al.* (2014), Wakefield (2007) and Fong *et al.* (2010), among other papers.

The following precision parameters were used: $\tau_u = 1/\sigma_u^2$ for the spatially structured random effect; $\tau_\phi = 1/\sigma_\phi^2$ for the temporally unstructured random effect; $\tau_\gamma = 1/\sigma_\gamma^2$ for the temporally structured random effect and $\tau_\delta = 1/\sigma_\delta^2$ for the space-time interaction term.

Spatio-temporal models above were then fitted with INLA methodology to the 2013-2016 HIV and AIDS data in Kenya.

3.4 Bayesian Model Estimation Methods

All disease mapping models discussed in this thesis are implemented using the Bayesian inference techniques. This section discusses the fundamentals of Bayesian inference and estimation. In Bayesian inference, the parameters within the likelihood model are allowed to be stochastic, that is, to have distributions. These distributions are called prior distributions and are assigned to the parameters before seeing the data. This allowance also makes the parameters in the prior distributions of the likelihood parameters to be stochastic. By so doing, hierarchical models are obtained. These models form the basis of inference under the Bayesian paradigm. The product of the likelihood (data) and the prior distributions for the parameter gives the so-called posterior distribution. This distribution describes the behavior of the parameters after observing the data and making the necessary prior assumptions.

For a simple likelihood model, the parameters are assumed to be fixed and maximum likelihood is often used to obtain the point estimate and associated variance for the parameters. This point estimate corresponds to the Standardized Mortality Ratio (SMR) for the case of simple disease mapping models. This is not true for Bayesian hierarchical disease mapping models because the parameters are no longer assumed to be fixed but stochastic.

Given the observed data, the parameter(s) of interest will be described by the posterior distribution which must be found and examined. For some simple models it is possible to find the exact form of the posterior distribution and to find explicit forms for the posterior mean or mode. However, most disease mapping models are complex and the resulting posterior distributions are not analytically tractable. Hence it is often not possible to derive simple estimators for parameters such as the relative risk. In this case posterior distribution is obtained via posterior sampling i.e., using simulation methods to obtain samples from the posterior distribution which then can be summarized to yield estimates of relevant quantities. Markov chain Monte Carlo (MCMC) algorithm has been the popular method for posterior distribution sampling in Bayesian applications until recently when approximation methods such as the Integrated Nested Laplace Approximation (INLA) were proposed. The following subsections describe the basics on the MCMC and INLA techniques.

3.4.1 Markov chain Monte Carlo

Markov chain Monte Carlo (MCMC) methods are a set of methods which use iterative simulation of parameter values within a Markov chain. The theory of MCMC was first developed as a tool for Bayesian posterior sampling starting in the early 1990s (Gelfand and Smith, 1990; Gilks *et al.*, 1993, 1996). Nowadays posterior sampling via MCMC is common and has been incorporated in a variety of software packages including WinBUGS, MlwiN and R. For good reviews on MCMC method, see Casella and George (1992), Dellaportas and Roberts (2003) and Robert and Casella (2005).

Consider a vector of observations $\boldsymbol{y}$ whose probability distribution or density function is indexed by a vector of unknown parameters $\boldsymbol{\theta}$. Then using Bayes theorem the posterior distribution of $\boldsymbol{\theta}$ is given by:

$$\pi(\boldsymbol{\theta} \mid \boldsymbol{y}) = \frac{p(\boldsymbol{y}|\boldsymbol{\theta}) \times p(\boldsymbol{\theta})}{p(\boldsymbol{y})} \tag{3.15}$$

where $p(\boldsymbol{\theta})$ is the prior probability distribution of $\boldsymbol{\theta}$ which represents the prior belief on $\boldsymbol{\theta}$; $p(\boldsymbol{y} \mid \boldsymbol{\theta})$ is the likelihood function which specifies the distribution of the data $\boldsymbol{y}$ given the prior belief; $p(\boldsymbol{y})$ is the marginal distribution of the data which is independent $\boldsymbol{\theta}$ and is treated as just a normalization constant. Thus the posterior distribution of $\boldsymbol{\theta}$ is often stated as:

$$\pi(\boldsymbol{\theta} \mid \boldsymbol{y}) \propto p(\boldsymbol{y} \mid \boldsymbol{\theta}) \times p(\boldsymbol{\theta}) \tag{3.16}$$

The marginal distribution of $\boldsymbol{y}$ is given by:

$$p(\boldsymbol{y}) = \begin{cases} \sum_{\boldsymbol{\theta} \in \Theta} p(\boldsymbol{y} \mid \boldsymbol{\theta}) p(\boldsymbol{\theta}), \text{ if } \boldsymbol{\theta} \text{ is discreate} \\ \int_{\boldsymbol{\theta} \in \Theta} p(\boldsymbol{y} \mid \boldsymbol{\theta}) p(\boldsymbol{\theta}) d\boldsymbol{\theta}, \text{ if } \boldsymbol{\theta} \text{ is continuous} \end{cases} \tag{3.17}$$

The goal of MCMC procedures is to generate random variables with stationary (or invariant or equilibrium) distributions that are similar to certain target distributions having probability distribution function $\pi(\boldsymbol{y})$. In the Bayesian inference technique, this target distribution is often the posterior distribution $p(\boldsymbol{\theta}|\boldsymbol{y})$. Thus, a sequence $\{\theta^{(1)}, \theta^{(2)}, ...\}$ of values derived from a Markov chain that has converged (i.e., has reached its invariant distribution) can be treated to be an estimate of the posterior density $\pi(\boldsymbol{\theta}|\boldsymbol{y})$ from which all the posterior summaries of interest are obtained.

The two standard procedures used in the MCMC technique are the Metropolis Hastings (MH) and the Gibbs sampler. The MCMC algorithm used in this thesis uses the Gibbs sampler algorithm. Gibbs Sampler was first developed by Geman and Geman (1984) for Bayesian image reconstruction and later proposed by Gelfand and Smith (1990) as a sampling procedure for simulating marginal distributions in a Bayesian estimation context. Casella and George (1992) gave a simple and good explanation of this algorithm. The Gibbs sampler is a special case of the MH technique in which the proposal distribution is generated from the conditional density of θ_i given all other $\theta^{'}$s, such that the resulting proposal value is accepted with probability 1.

The focus here is to simulate values from the posterior density $p(\boldsymbol{\theta} \mid \boldsymbol{y})$ of a generic p-dimensional vector of parameters $\boldsymbol{\theta} = \{\theta_1, ..., \theta_P\}$. The Gibbs sampler implements this by drawing values iteratively from all the conditional densities such that at the end it results in the transition from θ^t to θ^{t+1}. This algorithm is structured as follows (Coly *et al.*, 2019):

1. Begin with a set of initial values $\boldsymbol{\theta}^{(0)} = (\theta_1^{(0)}, ..., \theta_P^{(0)})'$ for all the parameters and set $t = 1$
2. Draw $\boldsymbol{\theta}^{(t)} = (\theta_1^{(t)}, ..., \theta_P^{(t)})'$ by

$$\theta_1^{(t)} \sim p(\theta_1 \mid \theta_2^{(t-1)}, ..., \theta_P^{(t-1)})$$
$$\theta_2^{(t)} \sim p(\theta_2 \mid \theta_1^{(t)}, \theta_3^{(t-1)}, ..., \theta_P^{(t-1)})$$
$$\vdots$$
$$\theta_d^{(t)} \sim p(\theta_d \mid \theta_1^{(t)}, , ..., \theta_{P-1}^{(t-1)})$$

3. Increase t by 1. i.e let $\boldsymbol{\theta}^{(t+1)} = (\theta_1^{(t+1)}, ..., \theta_P^{(t+1)})'$ and go back to step 2.

The Gibbs Sampler has gained a lot of popularity and attention in disease mapping and other epidemiological studies due to the availability of advanced softwares like WinBUGS which has made its implementation and application in a wide range of problems possible. Thus, in this thesis Gibbs Sampler is used.

3.4.2 Integrated Nested Laplace Approximation

The Integrated Nested Laplace Approximation (INLA) that has been recently developed for Bayesian inference is now becoming more popular than the famous MCMC algorithm in disease mapping applications. INLA provides efficient Bayesian inference for latent Gaussian Markov Random fields (GMRF) which is a special class of flexible hierarchical models that have been applied numerous applications.

The Spatial and spatio-temporal disease mapping models considered in this thesis fall into this class of GMRF and can be constructed in a three-stage Bayesian hierarchical framework. The first stage is the conditional distribution of observations $\boldsymbol{y}$; that is

$\pi(\boldsymbol{y} \mid \boldsymbol{x})$ where $\boldsymbol{x}$ represents the set of parameters. The second stage is the distribution of the set of parameters (may or may not be Gaussian) given the hyperparameters $\boldsymbol{\theta}$ which is the third stage; that is, $\pi(\boldsymbol{x} \mid \boldsymbol{\theta})$ with a precision matrix $\boldsymbol{R}$ (Rue and Held, 2005). For these models, the solutions for the posterior marginal distributions of the unknown parameters are not analytically tractable. Hence the parameter estimates are often obtained using MCMC technique, but the computations may take a longer time if samples are highly dependent. In contrast, INLA offers accurate Approximation to the posterior marginals of the model parameters and hyperparameters in a relatively shorter computation time. The following is a brief discussion on the steps for implementing INLA technique.

Let $\boldsymbol{x}$ denote the vector of all Gaussian variables and $\boldsymbol{\theta}$ the vector of hyperparameters. The objective is basically to approximate the posterior marginal distribution

$$\pi(x_i \mid \boldsymbol{y}) = \int_{\theta} \pi(x_i \mid \boldsymbol{\theta}, \boldsymbol{y}) \pi(\boldsymbol{\theta} \mid \boldsymbol{y}) d\boldsymbol{\theta} \tag{3.18}$$

of all parts of the GMRF by INLA using the finite sum:

$$\widetilde{\pi}(x_i \mid \boldsymbol{y}) = \sum_{k} \widetilde{\pi}(x_i \mid \boldsymbol{\theta}_k \, , \boldsymbol{y}) \widetilde{\pi}(\boldsymbol{\theta}_k \mid \boldsymbol{y}) \Delta_k \tag{3.19}$$

where $\widetilde{\pi}(x_i \mid \boldsymbol{\theta}_k \, , \boldsymbol{y})$ and $\widetilde{\pi}(\boldsymbol{\theta}_k \mid \boldsymbol{y})$ are respectively the Approximation of $\pi(x_i \mid \boldsymbol{\theta}, \boldsymbol{y}$ $)$ and $\pi(\boldsymbol{\theta} \mid \boldsymbol{y})$. This finite sum is evaluated at support points $\boldsymbol{\theta}_k$ using appropriate weights k .

From $\pi(\boldsymbol{x}, \boldsymbol{\theta}, \boldsymbol{y}) = \pi(\boldsymbol{x} \mid \boldsymbol{\theta}, \boldsymbol{y}) \times \pi(\boldsymbol{\theta} \mid \boldsymbol{y}) \times \pi(\boldsymbol{y})$ it follows that the posterior marginal marginal posterior density $\pi(\boldsymbol{\theta} \mid \boldsymbol{y})$ of the hyperparameters $\boldsymbol{\theta}$ can be obtained using a Laplace approximation

$$\widetilde{\pi}(\boldsymbol{\theta} \mid \boldsymbol{y}) \propto \frac{\pi(x, \boldsymbol{\theta}, \boldsymbol{y})}{\widetilde{\pi}_G(x \mid \boldsymbol{\theta}, \ \boldsymbol{y})} \mid_{x = \boldsymbol{x}^*(\boldsymbol{\theta})} \tag{3.20}$$

(Tierney and Kadane, 1986), where the denominator $\widetilde{\pi}_G(\boldsymbol{x} \mid \boldsymbol{\theta}, \boldsymbol{y})$ denotes the Gaussian approximation of $\pi(\boldsymbol{x} \mid \boldsymbol{\theta}, \boldsymbol{y})$ and $\boldsymbol{x}^*(\boldsymbol{\theta})$ is the mode of the full conditional $\pi(\boldsymbol{x} \mid \boldsymbol{\theta}, \boldsymbol{y})$ (Rue and Held, 2005).

The first part $\pi(x_i \mid \boldsymbol{\theta}, \boldsymbol{y})$ of the integral in (3.18) can be approximated using three different possible approaches. That is, a Gaussian, a full Laplace and a simplified Laplace approximation. The Gaussian approximation is fastest, but according to Rue and Martino (2007) this approach may not be accurate because of errors in locating the marginal posterior densities or errors arising due to lack of skewness or both. The Gaussian approximation can be enhanced by using a Laplace approximation to $\pi(x_i \mid \boldsymbol{\theta}, \boldsymbol{y})$ but this approach which is popularly known as ”full Laplace” is, however, time-consuming. Hence, Rue *et al.* (2009) came up with a simplified Laplace approximation approach which is not computationally cumbersome though slightly less accurate.

The Bayesian inference with INLA technique is implemented within the `R`-interface `R-INLA` using the `inla` package, which is a C program (Rue *et al.*, 2009). This program is based on the `GRMFLib-library`, which has got efficient algorithms for sparse matrices (Rue and Held, 2005). Here, the computations are speeded up by the implementation of parallel computing elements. The `inla` program has been incorporated within the `R` library (R Core Team, 2016). The software is available for free download at http://www.r-inla.org and can run in a Linux, MAC and Windows environment. For the analyses in this thesis, the `INLA` library built on the 3rd June 2014 was used.

The models in INLA can be ran by specifying the linear predictor of the model as a `formula` object in `R` using the function `f()` for the smooth effects and random effects. The interface is very flexible and it has options that allows different models and priors to be specified easily. Several authors (Gomez-Rubio *et al.*, 2014; Bivand *et al.*, 2015; Lindgren and Rue, 2015; Blangiardo and Cameletti, 2015) have given a summary of various spatial models incorporated in `R-INLA` latent effects that can be used to construct models. In this section, only an overview of the spatial models that will be used to fit the models considered in this chapter will be provided.

Spatial latent effects for areal data in `R-INLA` consist of a prior distribution which assume a multivariate normal distribution with zero mean and precision matrix $\tau \boldsymbol{C}$, where τ is a precision parameter and $\boldsymbol{C}$ is a symmetric square structural matrix which determines the spatial correlation and it can assume different forms to induce different types of spatial interaction. When $\boldsymbol{C}$ is completely specified, like in the case of spatio-temporal interaction effect, the `"generic0"` model is implemented and it defines a multivariate normal prior distribution with zero mean and generic precision matrix $\boldsymbol{C}$ which is normally defined by the user.

For the case of spatially structured random effect, the `"besag"` and `"generic1"` models are used to implement, respectively, the intrinsic conditional autoregressive (ICAR) (Besag *et al.*, 1991) and Leroux conditional autoregressive (LCAR) (Leroux *et al.*, 1999) prior distributions. The `besag` model for the ICAR prior corresponds to a multivariate normal with zero mean and precision matrix $\tau\boldsymbol{Q}$, with the element d_{ij} defined by

$$q_{ij} = \begin{cases} n_i, \text{ if } i = j \\ -1, \text{ if } i \sim j \\ 0, \text{Otherwise} \end{cases} \tag{3.21}$$

where $n_{i,}$ is the number of neighbours of county i and $i \sim j$ indicates that counties i and j are neighbours. On the other hand, the LCAR prior, which forms the basis of the space-time disease mapping models discussed in this chapter, can not be obtained directly in `R-INLA`, but the `generic1` model can be used to introduce it easily. This model implements a multivariate normal distribution with zero mean and precision matrix $\tau\boldsymbol{L}$, with

$$\boldsymbol{L} = \left(I_n - \frac{\rho}{\lambda_{\max}}\boldsymbol{A}\right) \tag{3.22}$$

where $\lambda_{\max}$ is the largest eigenvalue of the structure matrix $\boldsymbol{A}$, which allows ρ to assume values between 0 and 1. To ensure that $\lambda_{\max} = 1$, Ugarte *et al.* (2014) defined the structure matrix $\boldsymbol{A}$ as $\boldsymbol{A} = \boldsymbol{I} - \boldsymbol{Q}$ where ijth element of matrix $\boldsymbol{A}$ is given by

$$a_{ij} = \begin{cases} -n_i + 1, \text{ if } i = j \\ 1, \text{ if } i \sim j \\ 0, \text{Otherwise} \end{cases} \tag{3.23}$$

Therefore, LCAR model proposed by Leroux *et al.* (1999) can be easily implemented in the `R-INLA` using a `generic1` model by letting $\boldsymbol{L} = \boldsymbol{I} - \boldsymbol{Q}$, so that $\boldsymbol{L} = (1 - \rho)I + \rho\boldsymbol{Q}$ with $\rho \in (0, 1)$.

In addition to the ICAR model implemented using the `besag` specification, `bym` model can be used to implement the sum of spatially structured and unstructured random effects described in the convolution model (Besag *et al.*, 1991). Similarly, for the spatially structured temporal random effects, the first and second order random walk priors are implemented using `"rw1"` and `"rw2"` models respectively. Finally, the identically independent random effects can be implemented using the `"iid"`model. In all these models, only the priors representing to the precision parameters (the inverse of the individual variances) should be specified.

In `R-INLA`, a call to function `inla()` is normally used to fit the model and it returns an `inla` object for the fitted model. This function enable for specification of various likelihood models (`family` object), computes marginal posterior densities of the latent effects and the hyperparameters by default. It also allows one to choose the strategy of integration for the Approximation with the object `control.inla`. In the analysis in this thesis, all spatio-temporal models were fitted using the Simplified Laplace Approximation strategy. Apart from the marginal distributions, marginal posterior densities for the linear predictor can also be obtained using the object `control.predictor`. For model choice and comparison, various indicators that include the effective number of parameters (pD) and the Deviance Information Criterion (DIC) are also provided within `INLA` via the object `control.compute`.

3.5 Bayesian Model Comparison

There are several approaches to assess model fit for comparison. In this thesis, the following two methods are used for comparing models: the deviance information criterion (DIC) and the mean squared predictive error (MSPE).

Let $p(\mathbf{y} \mid \theta)$ be a probability model. Spiegelhalter *et al.* (2002) defined Bayesian deviance $D(\theta)$ used for determining model goodness of fit as;

$$D(\theta) = 2\log f(\mathbf{y}) - 2\log p(\mathbf{y} \mid \theta) \tag{3.24}$$

where $f(\mathbf{y})$ is some fully specified standardizing term. For measuring model complexity, they give the effective number of parameters pD as;

$$pD = -D(E[\theta \mid \mathbf{y}]) + E[D(\theta \mid \mathbf{y})] \tag{3.25}$$

where $D(E[\theta \mid \mathbf{y}$ is the deviance of the posterior means and $E[D(\theta \mid \mathbf{y})]$ is posterior mean of the deviance.

Thus to measure both the model goodness of fit and complexity, Spiegelhalter *et al.* (2002) proposed the use of the deviance information criterion (DIC) defined as the sum of the effective number of parameters and the posterior mean of the deviance:

$$DIC = pD + E[D(\theta \mid \mathbf{y})] \tag{3.26}$$

The best model according to this criterion is the one with the smallest value of DIC. When MCMC is implemented in WinBUGS software, the values of the posterior mean of the deviance $E[D(\theta \mid \mathbf{y})]$, deviance of the posterior means $D(E[\theta \mid \mathbf{y})$, effective number of parameters pD and the DIC are typically provided in the output when DIC is set in the inference menu before running the model update.

To determine the best model for prediction, Gelfand and Ghosh (1998) proposed a loss function based method in which the observed data are compared to the predicted data from the fitted model. Let y_i^{pr} be the ith predicted data item from posterior sample that has converged. Suppose the current parameters at iteration j are given, say, by $\theta^{(j)}$. Then;

$$p(y_i^{pr} \mid \mathbf{y}) = \int p(y_i^{pr} \mid \theta^{(j)})\pi(\theta^{(j)} \mid \mathbf{y})d\theta^{(j)} \tag{3.27}$$

Hence the jth iteration can produce y_{ij}^{pr} from $p(y_i^{pr} \mid \theta^{(j)})$. The predictive values obtained have marginal distribution $p(y_i^{pr} \mid \mathbf{y})$. In the case of a Poisson distribution, this basically requires generation of counts as $y_{ij}^{pr} \leftarrow$ Poisson$(e_i\theta_i^{(j)})$.

A loss function is always assumed where $L_0(y, y^{pr}) = f(y, y^{pr})$. The squared error loss could be an appropriate choice of loss. This is defined as:

$$L_0(y, y^{pr}) = (y - y^{pr})^2 \tag{3.28}$$

The average loss across all the observations can be captured by *mean squared predict-*

ive error (MSPE) which is basically given by the average of the item-wise squared error loss. The MSPE is defined by (Lawson and Lee, 2017):

$$MSPE = \sum_i \sum_j \left(y_i - y_{ij}^{pr}\right)^2 / (G \times m) \tag{3.29}$$

where m and G are respectively the number of observations and the sampler sample size. It is noted here that, the smaller the value of MSPE, the more predictive the model is.

An alternative approach for checking the model predictive behaviour could be to measure the absolute error loss in the data using the *mean absolute predictive error* (MAPE) (Coly *et al.*, 2019)

$$MAPE = \sum_i \sum_j \left|y_i - y_{ij}^{pr}\right| / (G \times m) \tag{3.30}$$

CHAPTER FOUR

RESULTS AND DISCUSSIONS

4.1 Application of Skew-Random Effects Model to HIV and AIDS Data

In this section the disease mapping models with skew spatially unstructured random effects are applied to the analysis of 2016 HIV and AIDS incidence data in $n = 47$ Kenya counties. The data was collected by the Ministry of Health, Kenya and was extracted from the Kenya Demographic and Health Survey of 2017. In particular, Poisson log-skew normal (PLSN) and Poisson log-skew- t (PLST) models are compared with their corresponding symmetric models Poisson log-normal (PLN) and Poisson log-t (PLT).

Model estimation was carried out using a Bayesian approach. All parameters in the models were assigned prior distributions. In these models, a non-informative normal prior was assigned to the fixed effect coefficient β_0. The shape parameter λ was given a gamma prior distribution, and the variance parameters were assigned inverse gamma distributions. The models were implemented using WinBUGS (Spiegelhalter *et al.*, 2007). For each model, 6,000 Markov chain Monte Carlo (MCMC) iterations were ran, with the initial 2,000 discarded to cater for the burn-in and thereafter keeping every tenth sample value. The 4,000 iterations left were used for assessing convergence of the MCMC and parameter estimation. MCMC convergence were monitored using trace plots (Gelman *et al.*, 2004).

The analysis give the following parameter estimates and the goodness of fit measures, as presented in Table 4.1.

Table 4.1: *Parameter estimates for the models*

Model	β_0	σ_u	σ_v	k	δ	pD	DIC	MSPE
PLN	-0.0550	-	0.8692	-	-	75.302	693.13	50440
PLSN	0.6245	-	0.4809	-	-1.533	-48.374	618.40	50770
PLT	-0.0825		0.4848	3.636	-	-37.230	551.80	50260
PLST	0.2099	-	0.4474	5.918	-29.79	-199.963	390.01	50480

From Table 4.1, it can be seen that the standard deviation parameter σ_v estimates are smaller for skewed models than the ones for the corresponding symmetric models.

The estimates of the skewness parameter δ are negative in both the skew-normal and skew-t models. This confirms that the 2016 Kenya HIV and AIDS cases (response variable) is skewed to the left. Further more, the 95% credible limits for the skewness parameter δ were obtained as $(-1.682, -1.426)$ and $(-32.57, -27.25)$ for the skew-normal and skew-t models respectively. This shows the parameter δ is significant under both these two models¿ This indicates that the skewness parameter is important in modeling the 2016 Kenya HIV and AIDS data.

For model comparison, the effective number of parameters (pD) and the deviance information criterion (DIC) proposed by (Spiegelhalter *et al.*, 2002) were computed. The best fitting model is one with the smallest DIC value. From the DIC values in Table 4.1, it clear that models whose unstructured random effects follow asymmetric skewed distributions have quite small DIC values in comparison to the models with corresponding symmetric distributed unstructured random effects. This confirms that the skew-normal and skew-t prior models produce better results than the popular symmetric lognormal and student t- prior models. In particular, Poisson log-skew-t model has the smallest DIC value and hence is the best model in terms of a trade-off between model fit and complexity. The respective WinBUGS code for this model is provided in Appendix 2. On the other hand, the overall loss across the data was assessed by the use of the Mean Squared Predictive Error (MSPE) (Lawson and Lee, 2017), which is an average of the item-wise squared error loss. The best model for prediction is the one with the lowest MSPE value. The Poisson log- t- model has the lowest MSPE value as compared to the other models indicating that the it has a good predictive behaviour as compared to the other models.

Figure 4.1 shows the spatial distribution of HIV and AIDS in Kenya in 2016 based on the best fitting model (Poisson log-skew-t). This is a map of relative risk and its corresponding credible interval.

4.2 Simulation Study for Skew-Random Effects models

To assess if models proposed are good at describing the true spatial variation and the relative risks near boundaries, data were simulated from a number of different possible relative risk models: (1) the case where only uncorrelated heterogeneity is present

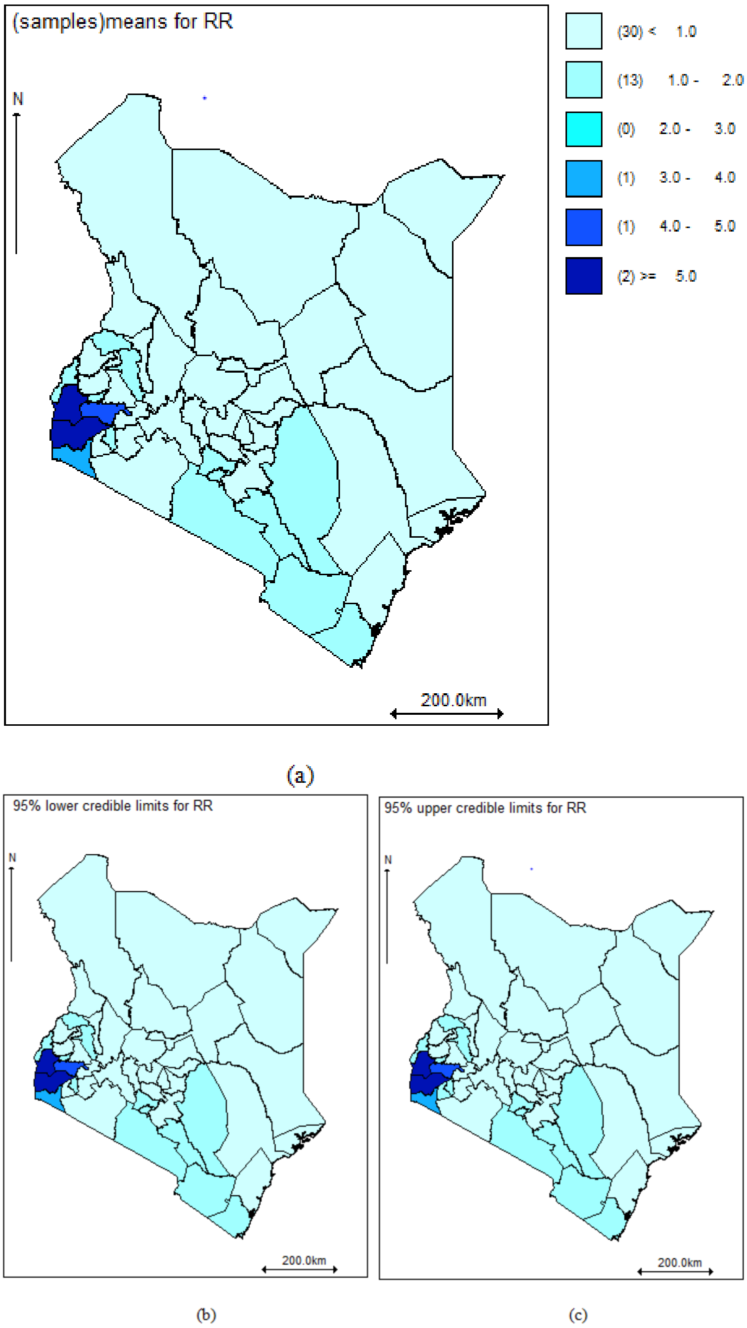

Figure 4.1: *HIV and AIDS relative risk map (a) and the 95% lower (b) and upper (c) credible limits maps for the Skew-t model*

(UH) (2) the case where only spatially correlated heterogeneity is present (CH) and (3) the case where both types of heterogeneity (CH+UH) are present simultaneously (convolution model). To achieve consistency with data analyses, the map of the 47 Kenya counties was used to simulate the relative risk distributions within. In addition, a set of fixed expected counts for the mapped area was required. The expected number of HIV cases from the 2017 Kenya Demographic and Health Survey for the year 2016 were used.

The simulated observed cases of HIV in counties were generated from a Poisson distribution:

$$Y_i \sim \text{Poisson}(E_i \omega_i) \tag{4.1}$$

where E_i is the expected number of HIV cases and ω_i is the unknown relative risk for county i during the study period.

To introduce the three different scenarios in terms of included heterogeneity, the relative risks were simulated as coming from three different models:

1) Lognormal uncorrelated heterogeneity (UH) model:

$$\begin{gathered} \omega_i = exp(v_i) \\ v_i \sim \text{Normal}(0, \sigma_v^2); \sigma_v^2 = \tfrac{1}{\tau_v^2} \end{gathered} \tag{4.2}$$

2) ICAR correlated heterogeneity (CH) model:

$$\begin{gathered} \omega_i = exp(u_i); \\ u_i \mid \boldsymbol{u}_{-i}, \sigma_u^2 \sim \text{Normal}\left(\bar{\mu}, \sigma_i^2\right); \\ u_i = \tfrac{1}{n_i} \sum_{i \sim j}^{n} u_j, \sigma_i^2 = \tfrac{\sigma_u^2}{n_i}, \sigma_u^2 = \tfrac{1}{\tau_u^2} \end{gathered} \tag{4.3}$$

where n_i is the number of neighbours of the ith area; $i \sim j$ indicates that areas i and j are neighbours. The spatially-structured heterogeneity (u_i) values were sampled directly from WinBUGS.

3) Convolution (UH+CH) model:

$$\begin{aligned}
\omega_i &= exp(v_i + u_i); \\
v_i &\sim \text{Normal}(0, \sigma_v^2); \sigma_v^2 = \tfrac{1}{\tau_v^2}; \\
u_i \mid \boldsymbol{u}_{-i}, \sigma_u^2 &\sim \text{Normal}\left(\bar{\mu}, \sigma_i^2\right); \\
u_i &= \tfrac{1}{n_i} \sum_{i \sim j}^{n} u_j, \sigma_i^2 = \tfrac{\sigma_u^2}{n_i}, \sigma_u^2 = \tfrac{1}{\tau_u^2}
\end{aligned} \tag{4.4}$$

Exactly the same values as simulated in (1) and (2) above were both included in this model.

Data were simulated only for the case where the spatially-structured heterogeneity was assumed to be largely present in the data while there was only a little uncorrelated heterogeneity. This was achieved by setting $\tau_v^2 = 0.5$ and $\tau_u^2 = 5$ (Neyens *et al.*, 2012).

The observed counts data were simulated under these three models and then, regardless of the sampling model, the 4 models described in Section 3.1 were fitted: Poisson log-normal (PLN), Poisson log-skew normal (PLSN), Poisson log-t (PLT) and Poisson log-skew- t (PLST) models. To improve on precision, 200 simulations were run using the three scenarios above.

Model selection was done by using Mean Squared Error (MSE), defined as:

$$MSE = \frac{1}{n-1} \sum_{i=1}^{n} (\hat{\omega}_i - \omega_i)^2 \tag{4.5}$$

where $i = 1, ..., n$ with $n = 47$ which was averaged over the 200 simulated data sets. The DIC goodness of fit measures were also compared for the simulated models.

Table 4.2 shows the MSE values obtained for the four analyzed models under the three different scenarios.

Table 4.2: *Simulation study: average MSE values (bold = lowest)*

Analyzed model	lognormal (UH)	ICAR (CH)	Convolution (UH+CH)
PLN	0.0145	0.0147	0.0142
PLSN	00.0142	0.0141	0.0145
PLT	0.0143	**0.0139**	0.0143
PLST	**0.0140**	0.0145	**0.0138**

Although the results presented in Table 4.2 do not show large differences in average MSE between models, they are consistent with the results seen in the analysis of real data. For the case where uncorrelated heterogeneity (UH) is present (Lognormal and Convolution columns), the Poisson log skew-t (PLST) model performs fairly well and if only spatially correlated heterogeneity (CH) is present, Poisson log-t (PLT) model performs well.

Table 4.3 show the DIC values obtained for the four analyzed models under the three different scenarios.

Table 4.3: *Simulation study: DIC values (bold = lowest)*

Analyzed model	Lognormal (UH)	ICAR (CH)	Convolution (UH+CH)
PLN	943.8	944.7	943.8
PLSN	929.4	883.9	899.3
PLT	920.9	897.6	869.7
PLST	**882.43**	**784.5**	**805.6**

In terms of DIC, the PLST model is the best fitting model to the simulated data in all the three scenarios of generating the relative risks. This agrees with the analysis of the real HIV and AIDS data set presented in Section 4.1 above.

4.3 Application of Skew-t Spatial Combined Random Effects model to HIV and AIDS Data

In this section the skew spatial combined random effects model is used to analyze 2016 HIV and AIDS incidence data for $n = 47$ Kenya counties. The data has been described in Section 1 of Chapter One. An overview of summary statistics is given in Table 4.4.

Table 4.4: *Summary statistics for 2016 HIV and AIDS in Kenya*

Statistic	Value
Mean	25689
Variance	577357958
Minimum	413
Maximum	112226

Table 4.4 shows that the variance of the HIV and AIDS counts is very large, an indication that there could be extra-Poisson variation in the data set. Standardizing

(Inskip *et al.*, 1983) these observed counts for county population sizes and age distributions to provide the expected counts solves a part of the problem. It is also very likely that part of the remaining variability can be explained by correlations through space on one hand but also by spatially uncorrelated overdispersion (e.g., caused by not standardizing for an important but still unknown factor) on the other hand.

In other words, estimates of the well-known Standardized Incidence Rates, $\text{SIR}_i = Yi/Ei$ (Figure 4.2), may be overly simplistic and models which include random effects for both uncorrelated heterogeneity (UH) and correlated heterogeneity (CH) will probably be better suited for these data.

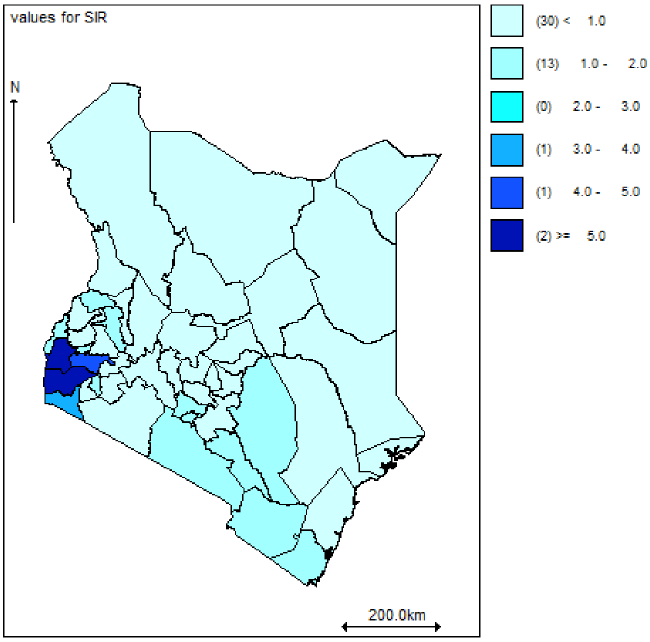

Figure 4.2: *Standardized incidence rates for 2016 HIV and AIDS in Kenya*

The skew-t conditional autoregressive combined (STCARCOM) model proposed in this thesis was compared to the existing classical disease mapping models: Poisson-gamma (PG), Poisson-lognormal (PLN), intrinsic conditional autoregressive correlated heterogeneity (ICAR CH), convolution (CON), and the skew-t conditional autoregressive (STCAR) using the 2016 HIV and AIDS incidence data in $n = 47$ Kenya counties.

Model estimation was carried out using Bayesian approach using the hierarchical specification where all model parameters are assigned prior distributions. For the hyperparameters a and b in the gamma distribution of Poisson-gamma model, pCAR combined model and STCAR combined model, $a \sim \exp(1)$ and $b \sim$ Gamma$(0.1, 1)$ were used as suggested by Lawson *et al.* (2013). The prior distributions of the variance parameters are $1/\sigma_v^2$ ~Gamma$(0.5, 0.0005)$ and $1/\sigma_u^2$ ~Gamma$(0.5, 0.0005)$ Kelsall and Wakefield (1999); a uniform prior distribution was used for the spatial smoothing parameter ρ, that is, $\rho \sim U(0, 1)$ (Kelsall and Wakefield, 2002); the skewness parameter δ was given zero mean Gaussian distribution $\delta \sim N(0, 0.01)$ (Branco and Dey, 2001) while the intercept term β_0 was assigned a weakly informative Gaussian prior distribution $\beta_0 \sim N(0, 0.000001)$ (Arab, 2015); and finally the parameter k representing the degrees of freedom was assigned a truncated exponential prior distribution $p(k) \propto \lambda_0 \exp^{\lambda_0 k} I\{k > 2\}$ with $\lambda_0 = 0.1$ in order to favor heavy tails (Nathoo and Ghosh, 2012).

Models were implemented using WinBUGS version 1.4 (Spiegelhalter *et al.*, 2007; Ntzoufras, 2011). For each model, 6,000 Markov chain Monte Carlo (MCMC) iterations were ran, with the initial 2,000 discarded to cater for the burn-in and thereafter keeping every tenth sample value. The 4,000 iterations left were used for assessing convergence of the MCMC and parameter estimation. MCMC convergence were monitored using trace plots, see Gelman *et al.* (2004). For model comparison and goodness-of-fit (GOF), the deviance information criterion (DIC) proposed by (Spiegelhalter *et al.*, 2002) was adopted. The best fitting model is one with the smallest DIC value. On the other hand, the overall loss across the data was assessed by the use of the Mean Squared Predictive Error (MSPE). The best model for prediction is the one with the lowest MSPE value.

The results are given in Table 4.5 below.

Table 4.5: *Parameter estimates for the models*

Model	$\boldsymbol{\beta_0}$	$\boldsymbol{\sigma_v}$	$\boldsymbol{\sigma_u}$	$\boldsymbol{\rho}$	k	δ	pD	DIC	MSPE
PG	-	0.862	-	-	-	-	47.01	636.51	51060
PLN	-0.055	0.8692	-	-	-	-	75.30	693.13	50440
ICAR CH	-0.210	-	1.241	-	-	-	133.23	928.30	76130
CON	-0.225	0.240	1.218	-	-	-	67.05	676.60	50490
STCAR	0.040	-	75.2	0.124	8.07	-0.370	6.04	595.77	50560
STCARCOM	0.028	0.138	96.25	0.137	13.14	0.142	-103.04	487.10	50310

In terms of DIC, the models with the gamma overdispersion and skew-t random effect terms are favored. It can be seen that the PG, STCAR and STCARCOM have similar smaller DIC values as compared to the PLN, ICAR CH and CON models, showing that the gamma- and skew-t random efffects improve the model fit as compared to the normally distributed random effects. Considering the relative risk (RR) estimates presented in Appendix 1, it is shown that the credibility intervals for RR differ from 1 for all the counties. This indicates presence of important spatial heterogeneity in the data. It is noted here that the STCAR and STCARCOM models have the smaller pD values, an evidence that these models are less parameterized as compared to the other models. The proposed STCARCOM model has the smallest values for both DIC and MSPE, indicating that this proposed model is the best in terms of model fit and predictive behaviour. The respective WinBUGS code for this model is provided in Appendix 3.

Similar conclusions are drawn from the parameter estimates, in which the estimated values for the intercept β_0, the standard deviations of the spatially-unstructured and spatially-structured random effects σ_v and σ_u are shown. σ_v comes from either the gamma distributed random effect in the PG and STCARCOM models or from the log-normal distributed random effect in the PLN, ICAR CH and convolution models, while σ_u comes from either the ICAR normal random effects in the ICAR CH and convolution models or the pCAR normal random effects in the STCAR and STCARCOM models.

4.4 Simulation study for Skew-t Spatial Combined Random Effects Model

For the skew-t spatial combined random effects model analysis, the simulation procedures presented in Section 4.2 for skew random effect models were also used. That is, data were also simulated from a number of different possible relative risk models: (1) the case where only uncorrelated heterogeneity is present (UH) (2) the case where only spatially correlated heterogeneity is present (CH) and (3) the case where both types of heterogeneity (CH+UH) are present simultaneously (convolution model). However, in this case the three scenarios were simulated separately for two settings, setting A where the data contained a large amount of uncorrelated heterogeneity and only little spatially-structured heterogeneity on one hand and setting B where the spatially-structured heterogeneity was largely present in the data while there was only little uncorrelated heterogeneity on the other. To simulate only a little relatively large amount of UH (setting A), $\tau_v^2 = 0.05$ was used while in the setting with little UH (setting B), $\tau_v^2 = 0.5$ was chosen (Neyens *et al.*, 2012). Only a little amount of CH (setting A) was simulated by setting $\tau_u^2 = 500$ while a relatively high amount of CH (setting B) was simulated by setting $\tau_u^2 = 5$ (Neyens *et al.*, 2012).

Again, 200 simulations of both settings A and B were run, separately, using the three scenarios above. The simulated observed cases of HIV were analyzed with six models: Poisson-gamma (PG), Poisson-lognormal (PLN), intrinsic conditional autoregressive correlated heterogeneity (ICAR CH), convolution (CON), skew-t conditional autoregressive (STCAR) and the skew-t conditional autoregressive combined (STCARCOM). The MSE was also used for model selection.

Table 4.6 show the MSE values obtained for the six models analyzed under the two settings for the three different scenarios.

Table 4.6: *Simulation study: average MSE values (bold = lowest) for setting A (large UH, small CH) and setting B (small UH, large CH)*

	Setting A			Setting B		
Analyzed model	Log-normal (UH)	ICAR (CH)	Convolution (UH+CH)	Log-normal (UH)	ICAR (CH)	Convolution (UH+CH)
PG	0.0140	0.0144	0.0142	0.0146	**0.0140**	0.0144
PLN	0.0146	0.0149	0.0147	0.0145	0.0151	0.0147
ICAR CH	0.0416	0.0433	0.0419	0.0418	0.0413	0.0419
CON	0.0150	0.0153	0.0148	0.0148	0.0151	0.0146
STCAR	0.0145	0.0147	0.0144	**0.0137**	0.0148	0.0145
STCARCOM	**0.0136**	**0.0142**	**0.0138**	0.0145	0.0147	**0.0143**

The results presented in Table 4.6 do not show large differences in average MSE between models, but are again consistent with the results obtained in the analysis of real data: the skew-t spatial combined (STCARCOM) model behaves particularly well when there is a large amount of uncorrelated heterogeneity (UH) present in the data (setting A). In this setting, average MSE values are slightly lower for the STCARCOM for the case in which only UH was present in the data (Log-normal and Convolution columns). This is also consistent with previous observations, which state that the STCARCOM model does well when there is a large amount of overdispersion or uncorrelated heterogeneity, but not necessarily when a map contains a lot of spatially induced extra-variance (correlated heterogeneity).

Finally, Table 4.7 show the DIC values obtained for the six models analyzed under the two settings for the three different scenarios.

Table 4.7: *Simulation study: DIC values (bold = lowest) for setting A (large UH, small CH) and setting B (small UH, large CH)*

	Setting A			Setting B		
Analyzed model	Log-normal (UH)	ICAR (CH)	Convolution (UH+CH)	Log-normal (UH)	ICAR (CH)	Convolution (UH+CH)
PG	692.4	686.8	690.5	715.2	710.2	712.2
PLN	855.6	803.4	840.5	778.5	874.5	902.4
ICAR CH	927.2	932.4	929.6	930.1	926.3	928.7
CON	746.5	743.5	740.4	754.7	743.8	748.3
STCAR	701.3	711.3	702.6	725.5	720.6	717.1
STCARCOM	**670.8**	**652.6**	**675.7**	**662.8**	**687.4**	**673.5**

In terms of DIC, the STCARCOM model is the best fitting model to the simulated data in all the three scenarios of generating the relative risks under setting A. On the other hand, when there is very little or zero extra-variance present in the data, the skew-t spatial combined model, will analyze the data not as good as the normal distribution-based solutions. This also confirms the results obtained in the analysis of real data in which the skew-t spatial combined (STCARCOM) was the best fitting model.

4.5 Spatio-temporal Variation of HIV and AIDS Infection in Kenya

The parametric linear time trend and the non-parametric dynamic time trend models were applied to to the HIV and AIDS data in Kenya for the period 2013-2016. The models were implemented using Integrated Nested Laplace Approximation (INLA). The corresponding `R-INLA` codes for spatio-temporal analysis of HIV and AIDS in Kenya is provided in Appendix 4.

The spatial patterns for HIV and AIDS cases in Kenya for the period 2013-2016 are given in Figure 4.3.

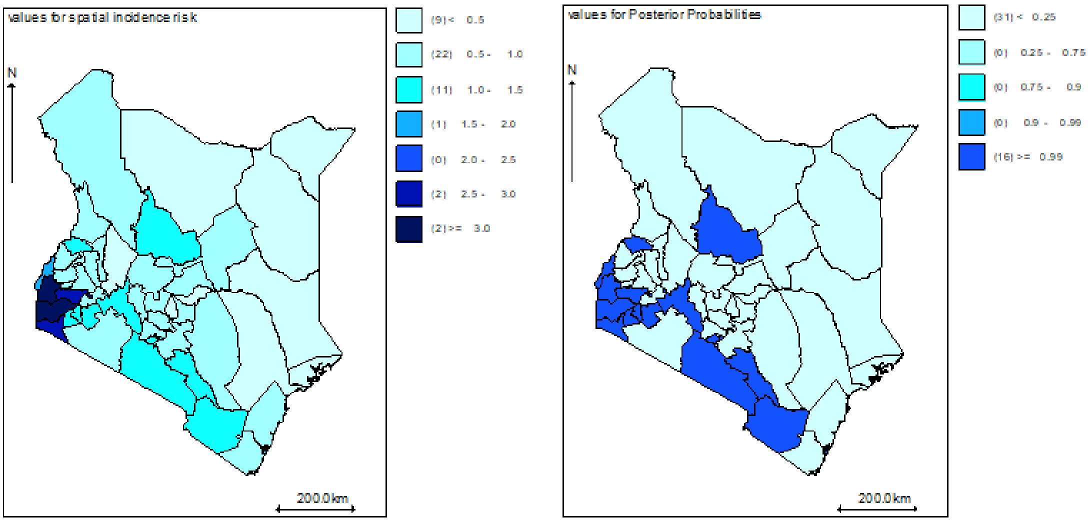

(a) (b)

Figure 4.3: *The spatial pattern of HIV and AIDS incidence risks* $\zeta_i = exp(u_i)$ *(a); Posterior probabilities* $P(\zeta_i > 1|Y)$ *(b)*

The left figure (a) presents the spatial incidence risk ($\widehat{\zeta_i} = \exp(\widehat{u}_i)$) associated to each county and constant along the period while the right figure (b) presents the posterior probability that the spatial risk is greater than 1 ($p = P(\zeta_i > 1 \mid Y)$). Probabilities above 0.9 point towards high risk areas. Some discussions about reference thresholds in relative risks and cut-off probabilities can be obtained in Richardson *et al.* (2004), Ugarte *et al.* (2009a) and Ugarte *et al.* (2009b). It is clear from this figure that there is a higher risk of HIV and AIDS infection in the counties to the Western region of Kenya as compared to the other counties. In particular, Homa Bay, Siaya, Migori and Kisumu counties show high relative risks.

Figure 4.4 shows the posterior mean of the main time effect together with its 95% credibility interval. This plot show a positive increment in the risk of HIV and AIDS for every subsequent year.

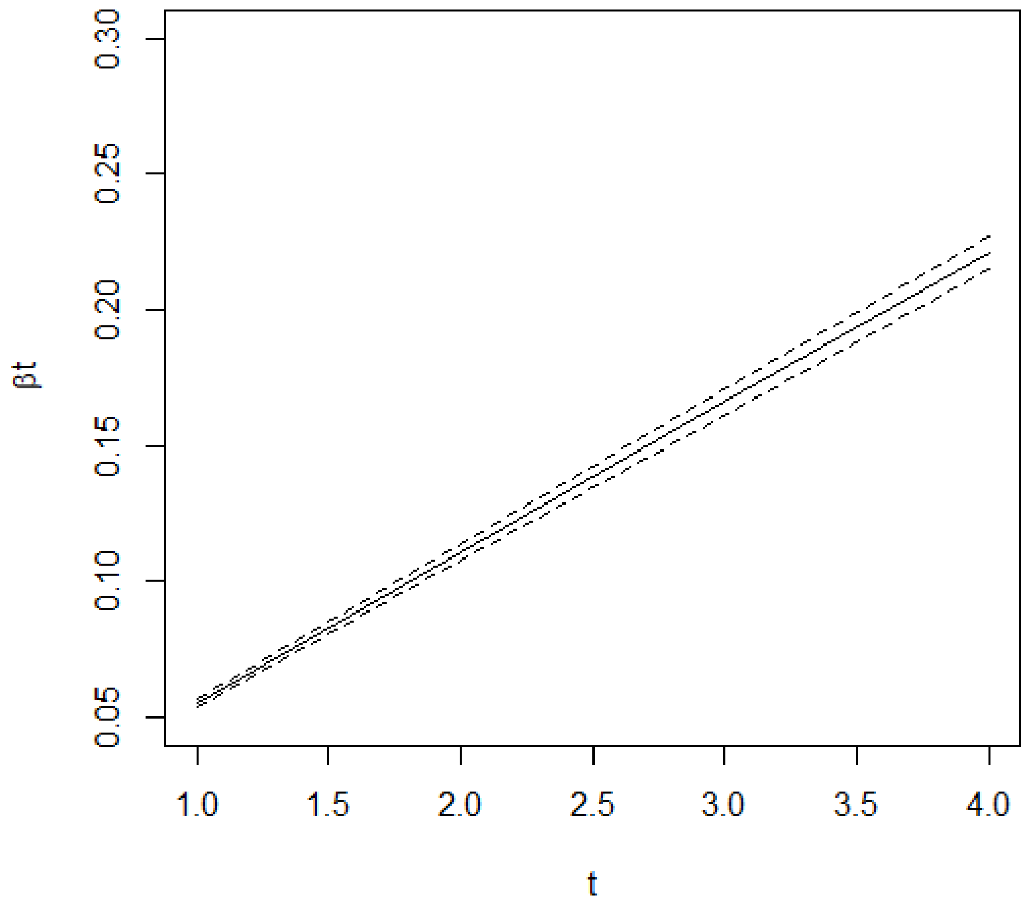

Figure 4.4: *Global linear temporal trend of HIV and AIDS incidence risks. Solid line: posterior mean for βt; Dashed lines: 95% credibility intervals*

The temporal risk trend common to all counties are given in bottom figure in Figure 4.5 below.

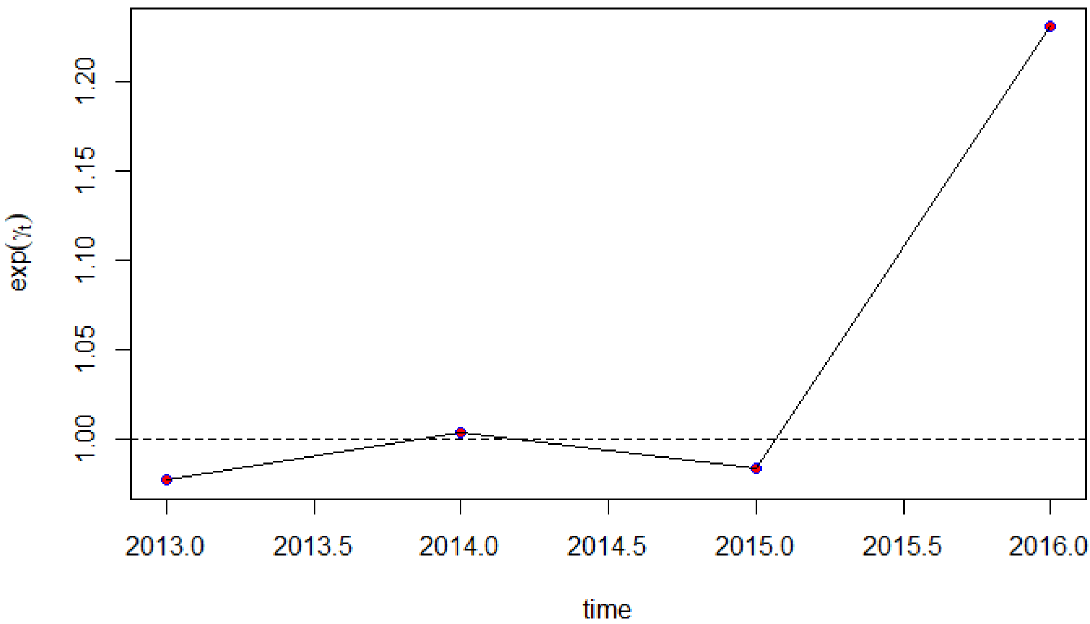

Figure 4.5: *Temporal trend of HIV and AIDS incidence risks*

Generally, there is an increasing trend in the whole period which indicates that there might be some factors affecting the whole country that produce an increase in risk along the period. There is a non-linear trend behavior of the temporal pattern over time, thus explaining the reason why the parametric linear trend models do not fit well to the HIV and AIDS data as compared to the non-parametric ones.

The specific temporal trends (in log scale) for four selected counties are shown in Figure 4.6.

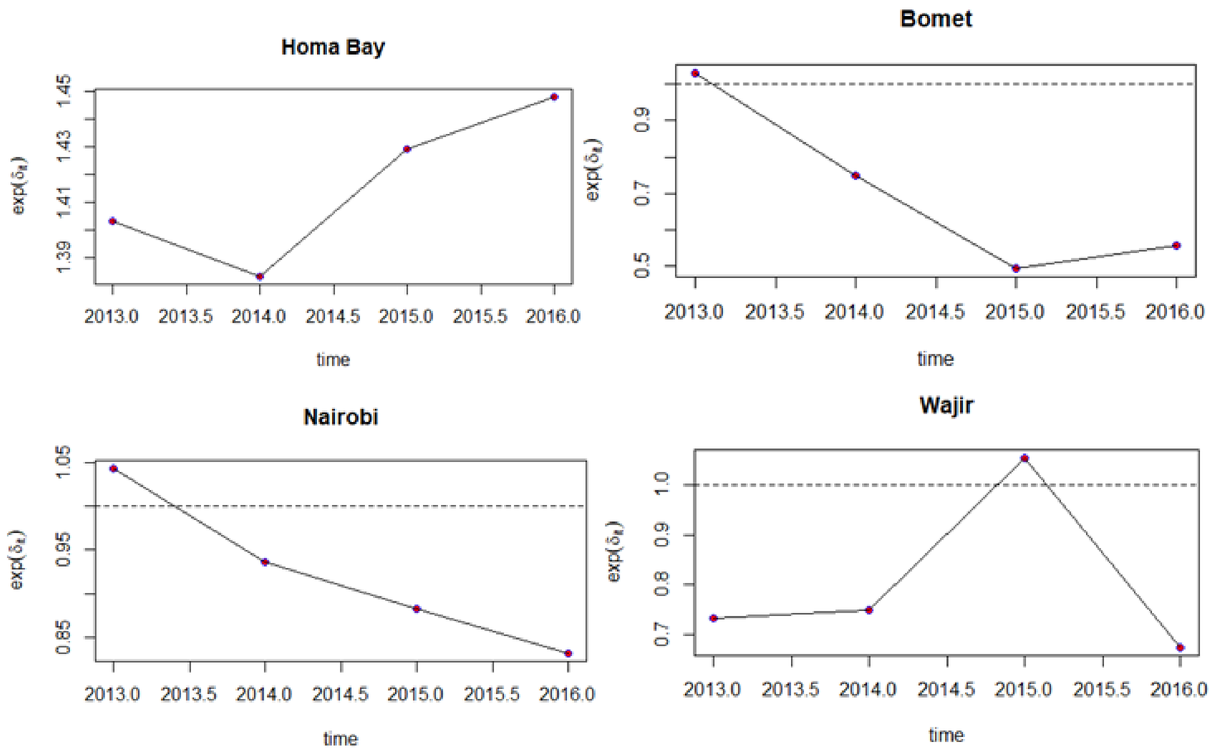

Figure 4.6: *Specific temporal trends for selected counties: Homa Bay, Bomet, Nairobi and Wajir.*

There is a clear differences among counties, which means including the interaction term in the model is appropriate.

The spatio-temporal interactions for the HIV and AIDS are given in Figures 4.7-4.10. It is clear from the information provided by the interaction maps that there is an increase in risk as the maps are getting darker with years. A number of counties in the Western region of Kenya show higher significant risk of HIV and AIDS as compared to other regions.

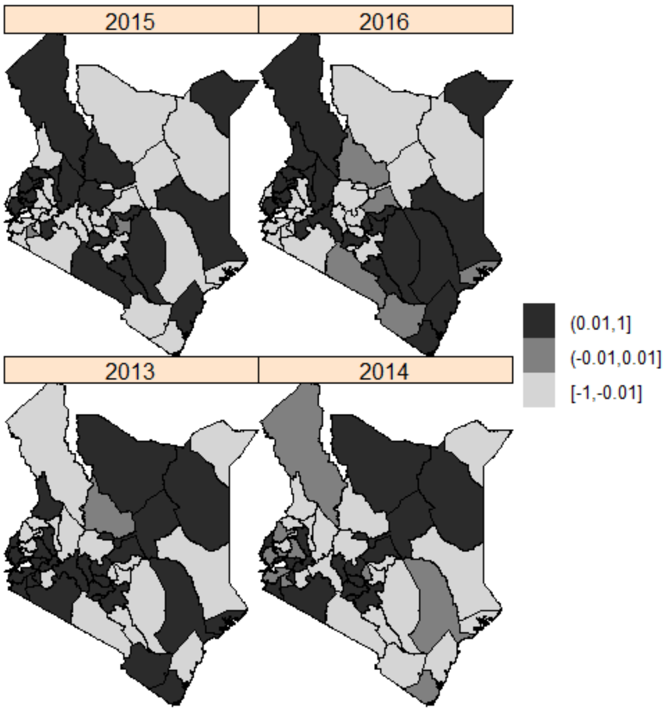

Figure 4.7: *Posterior mean of the spatio-temporal interaction δ_i: Type I Interaction*

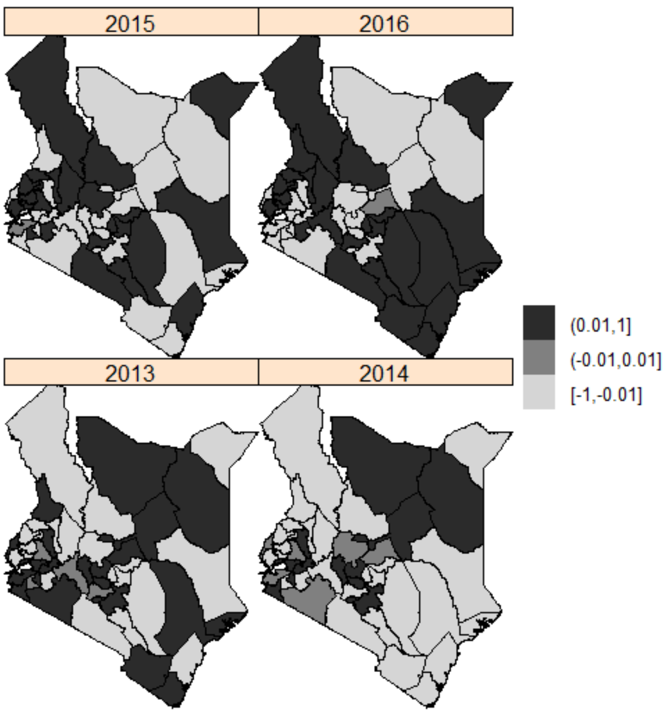

Figure 4.8: *Posterior mean of the spatio-temporal interaction δ_i: Type II Interaction*

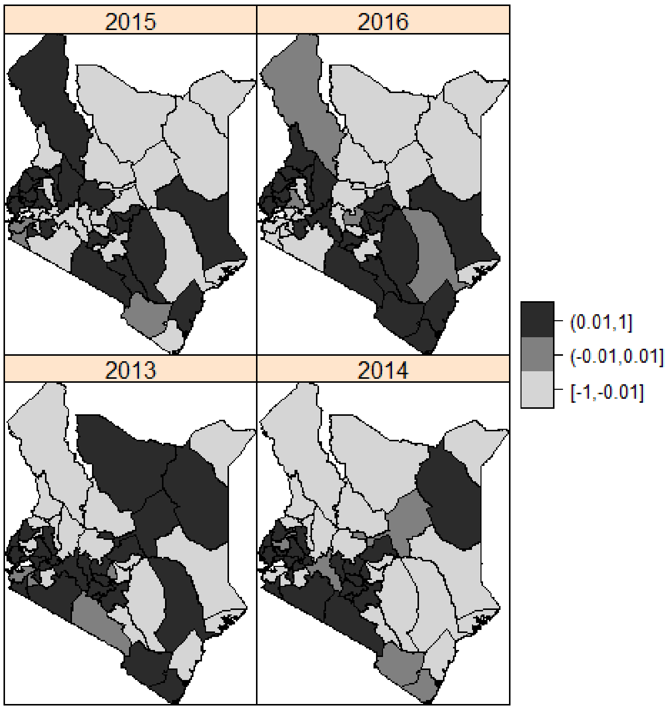

Figure 4.9: *Posterior mean of the spatio-temporal interaction δ_i: Type III Interaction*

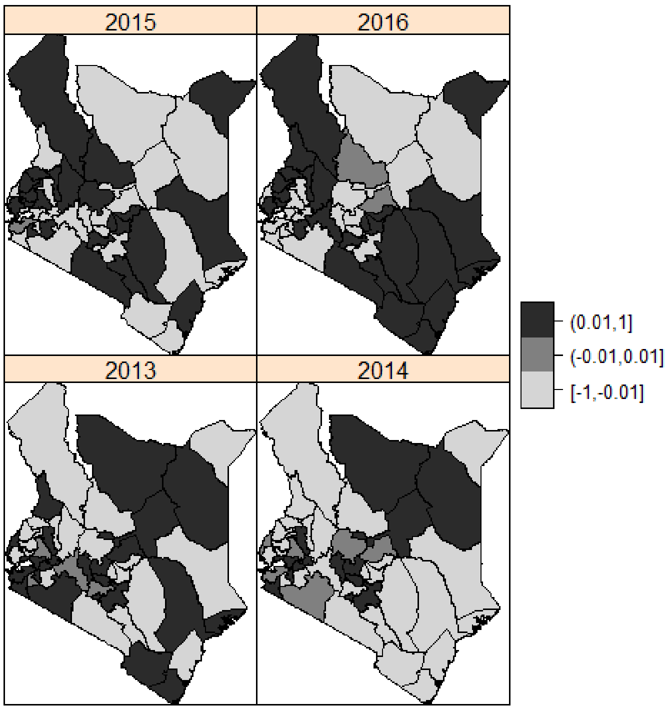

Figure 4.10: *Posterior mean of the spatio-temporal interaction δ_i: Type IV Interaction*

CHAPTER FIVE

CONCLUSION AND RECOMMENDATIONS

5.1 Conclusion

Disease maps play a key role in descriptive spatial epidemiology. Maps are useful for several purposes such as identification of areas with suspected elevations in risk, formulation of hypotheses about disease aetiology, and assessing needs for health care resource allocation.

A new model that relaxes the usual normality assumption on the spatially unstructured random effect by using the skew normal and skew-t distributions was introduced. In the analysis of 2016 HIV and AID data in Kenya, it was found out that models whose unstructured random effects follow skewed distributions generally perform better than models with normally distributed unstructured random effects.

Another flexible model known as skew-t spatial combined random effects model was also proposed. This new model combines a Poisson-gamma model with a spatially structured skew-t random effect in the same model is presented. In the analysis of 2016 HIV and AID data in Kenya, the skew-t spatial combined model provided a better alternative to the classical disease mapping models such as the popular Gaussian spatial models, with improved modeling capabilities when the data contain a large amount of uncorrelated heterogeneity. Simulation studies to assess the performance of the skew random effect distribution models and the skew-t spatial combined random effects model show that these proposed models perform better than the classical disease mapping models.

Spatio-temporal models which include linear time trend, non-parametric and space-time interactions models were also discussed. For modeling spatial random effect, Leroux CAR (LCAR) prior was used and Bayesian analysis implemented using INLA. INLA fit complex spatio-temporal models much faster than the Markov chain Monte Carlo (MCMC) algorithm. INLA also has an additional advantage since it can be easily implemented in the free software `R` using the package `R-INLA`. The INLA methodology also offers several quantities such as the effective number of parameters (pD) and the Deviance Information Criterion (DIC) for Bayesian model choice and comparison.

Finally, the analysis of the 2013-206 Kenya HIV and AIDS data shows that counties located in the Western region of Kenya show significantly higher risks as compared to the other counties. In particular, Homa Bay, Siaya, Migori and Kisumu counties show the highest risks. The reasons why these counties show high HIV and AIDS incidence risks is still a subject that needs investigation and further research is required.

5.2 Recommendations for Further Research

Future work will consider extensions of the models presented in Chapter Three. For example, the skew-t spatial combined model considered only explored the univariate case. Future research will focus on the multivariate count data case, which is also often encountered in many disease mapping problems. Furthermore, an extension of the skew-t spatial combined model to the spatio-temporal setting can be of interest as well. All the spatial and spatio-temporal models considered in this thesis are based on single disease modeling. Further research can consider extending these models to study multiple diseases. Finally, the models considered in this thesis were applied to the analysis of HIV and AIDS data. Further research can consider the application of these models to spatial and spatio-temporal analysis of other diseases as well.

REFERENCES

Abellan, J., Richardson, S. and Best, N. (2008). Use of space-time models to investigate the stability of patterns of disease. *Environmental Health Perspective*, 116(8), 1111–1119.

Agresti, A. (2002). *Categorical Data Analysis*. Wiley, New Jersey, 2nd edition.

Arab, A. (2015). Spatial and spatio-temporal models for modeling epidemiological data with excess zeros. *International Journal of Environmental Resesearch & Public Health*, 12, 10536–10548.

Assunção, R., Reis, I. and Oliveira, C. (2001). Diffusion and prediction of leishmaniasis in a large metropolitan area in brazil with a bayesian space-time model. *Statistics in Medicine*, 20, 2319–2335.

Azzalini, A. and Capitanio, A. (2003). Distributions generated by perturbation of symmetry with emphasis on a multivariate skew-t distribution. *Journal of the Royal Statistical Society, Series B*, 65, 367–389.

Banerjee, S., Carlin, B. P. and Gelfand, A. E. (2015). *Hierarchical Modeling and Analysis for Spatial Data*. Chapman & Hal, London: CRC Press.

Bernardinelli, L., Clayton, D. and Montomoli, C. (1995). Bayesian estimates of disease maps: How important are priors? *Statistics in Medicine*, 14, 2411–2431.

Besag, J., York, J. and Molli´e, A. (1991). Bayesian image restoration with two applications in spatial statistics (with discussion). *Annals of the Institute of Statistical Mathematics*, 43, 1–59.

Best, N., Thomas, A., Waller, L., Conlon, E. and Arnold, R. (1999). Bayesian models for spatially correlated disease and exposure data. In *Bayesian Statistics 6*, volume 6, pages 131–156. Proceedings of the Sixth Valencia International Meeting, Oxford University Press, USA.

Best, N., Richardson, S. and Thompson, A. (2005). A comparison of bayesian spatial models for disease mapping. *Statistical Methods of Medical Research*, 14, 35–59.

Bithell, J. (2000). A classification of disease mapping methods. *Statistics in Medicine*, 19, 2203–2215.

Bivand, R. S., Gomez-Rubio, V. and Rue, H. (2015). Spatial data analysis with r-inla with some extensions. *Journal of Statistical Software*, 63(20), 1–31.

Blangiardo, M. and Cameletti, M. (2015). *Spatial and Spatio-Temporal Bayesian Models with R-INLA*. John Wiley and Sons, Inc., New York.

Blangiardo, M., Cameletti, M., Baio, G. and Rue, H. (2013). Spatio-temporal bayesian models with r-inla. *Spatiotemporal Epidemiology*, 4, 33–49.

Botella-Rocamora, P., López-Quílez, A. and Martínez-Beneito, M. A. (2013). Spatial moving average risk smoothing. *Statistics in Medicine*, 32, 2595–2612.

Box, G. and Tiao, G. (1973). *Bayesian Inference in Statistical Analysis*. Addison-Wesley Pub. Co., UK.

Branco, M. and Dey, D. (2001). A general class of multivariate skew-elliptical distributions. *Journal of Multivariate Analysis*, 79, 99–113.

Breslow, N. E. and Clayton, D. G. (1993). Approximate inference in generalized linear mixed models. *Journal of the American Statistical Association*, 88, 9–25.

Casella, G. and George, E. I. (1992). Explaining the Gibbs sampler. *The American Statistician*, 46, 167–174.

CBS and MOH (2004). *Kenya Demographic & Health Survey 2003*. Calverton, Maryland: Central Bureau of Statistics (CBS) [Kenya], Ministry of Health (MOH) [Kenya] and ORC Macro.

Chen, J., Zhang, D. and Davidian, M. (2002). A monte carlo em algorithm for generalized linear mixed models with flexible random effects distribution. *Biostatistics*, 3 (3), 347–360.

Clayton, D. G. and Kaldor, J. (1987). Empirical bayes estimates of agestandardised relative risks for use in disease mapping. *Biometrics*, 43, 671–691.

Coly, S., Garrido, M., Abrial, D. and Yao, A. F. (2019). Bayesian hierarchical models for disease mapping applied to contagious pathologies. *Biological Research*.

Cressie, N. A. C. (1993). *Statistics for Spatial Data*. Wiley, CRC Press.

Dellaportas, P. and Roberts, G. O. (2003). An introduction to mcmc. In *Spatial statistics and computational methods (Aalborg, 2001), Volume 173 of Lecture Notes in Statistics*. Springer, New York.

Eberly, L. E. and Carlin, B. P. (2000). Identifiability and convergence issues for markov chain monte carlo fitting of spatial models. *Statistics in Medicine*, 19(1718), 2279–2294.

Elliott, P. and Wartenberg, D. (2004). Spatial epidemiology current approaches and future challenges. *Environmental Health Perspectives*, 112, 998–1006.

Fong, Y., Rue, H. and Wakefield, J. (2010). Bayesian inference for generalized linear mixed models. *Biostatistics*, 11, 397–412.

Gaetan, C. and Guyon, X. (2010). *Spatial Statistics and Modeling, Series in Statistics.* Springer.

Gelfand, A., Diggle, P., Fuentes, M. and Guttorp, P. (2010). *Handbook of Spatial Statistics*. Chapman & Hall/CRC, London.

Gelfand, A. and Ghosh, S. (1998). Model choice: A minimum posterior predictive loss approach. *Biometrika*, 85, 1–11.

Gelfand, A. E. and Smith, A. F. M. (1990). Sampling-based approaches to calculating marginal densities. *Journal of the American Statistical Association*, 85, 398–409.

Gelman, A., Carlin, J. B., Stern, H. S. and Rubin, D. (2004). *Bayesian Data Analysis*. Chapman and Hall, London, 2nd edition.

Geman, S. and Geman, D. (1984). Stochastic relaxation, Gibbs distributions, and the Bayesian restoration of images. *IEEE Transactions on Pattern Analysis and Machine Intelligence*, 6, 721–741.

Genton, M. G. (2004). *Skew-Elliptical Distributions and Their Applications: A Journey Beyond Normality*. Chapman & Hall/CRC.

Gilks, W., Richardson, S. and Spiegelhalter, D. (1996). *Markov chain Monte Carlo in Practice*. Boca Raton: Chapman & Hall/CRC.

Gilks, W., Richardson, S. and Spiegelhalter, D. (2005). *Markov chain Monte Carlo*. Wiley, Hoboken.

Gilks, W. R., Clayton, D. G., Spiegelhalter, D. J., Best, N. G., McNeil, A. J., Sharples, L. D. and Kirby, A. J. (1993). Modelling complexity: Applications of gibbs sampling in medicine. *Journal of the Royal Statistical Society*, B 55, 39–52.

Gomez-Rubio, V., Bivand, R. S. and Rue, H. (2014). Spatial models using laplace approximation methods. In Fischer, M. M. and Nijkamp, P. E., editors, *Handbook of Regional Science*, pages 1401–1417. Springer, Berlin.

Green, P. J. and Richardson, S. (2002). Hidden markov models and disease mapping. *Journal of the American Statistical Association*, 97, 1055–1070.

Held, L., Schrödle, B. and Rue, H. (2010). Posterior and cross-validatory predictive checks: A comparison of mcmc and inla. In *Kneib, T. and Tutz, G. (eds): Statistical modelling and regression structures.*, pages 91–110. Heidelberg.

Hu, B., Ning, P., Li, Y., Xu, C., Christakos, G. and Wang, J. (2020). Space-time disease mapping by combining bayesian maximum entropy and kalman filter: the bme-kalman approach. *International Journal of Geographical Information Science*, pages 1–24.

Inskip, H., Beral, V., Fraser, P. and Haskey, P. (1983). Methods for age-adjustments of rates. *Statistics in Medicine*, 2, 483–93.

Kassahun, W., Neyens, T., Molenberghs, G., Faes, C. and Verbeke, G. (2012). Modeling overdispersed longitudinal binary data using a combined beta and normal random-effects model. *Archives of Public Health*, 70(7).

Kelsall, J. and Wakefield, J. (1999). *Modelling spatial variation in disease risk; Technical Report*. Imperial College, London.

Kelsall, J. and Wakefield, J. (2002). Modeling spatial variation in disease risk: a geostatistical approach. *Journal of the American Statistical Association*, 97, 692–701.

Kim, H. and Mallick, B. (2004). A bayesian prediction using the skew gaussian distribution. *Journal of Statistical Planning and Inference*, 120, 85–101.

Kim, H., Sun, D. and Tsutakawa, R. K. (2002). Lognormal vs. gamma: Extra variations. *Biometrika Journal*, 44, 305–323.

KNBS (2010). *Kenya Demographic & Health Survey 2008-09*. Calverton, Maryland: Kenya National Bureau of Statistics (KNBS) [Kenya] and ICF Macro.

KNBS, NASCOP, NACC, KEMRI and NCAPD (2015). *Kenya Demographic & Health Survey 2014*. Rockville, MD, USA: Kenya National Bureau of Statistics, Ministry of Health/Kenya, National AIDS Control Council/Kenya, Kenya Medical Research Institute, National Council for Population and Development/Kenya, and ICF International.

Knorr-Held, L. (2000). Bayesian modelling of inseparable space-time variation in disease risk. *Statistics in Medicine*, 19(18), 2555–2567.

Knorr-Held, L. and Besag, J. (1998). Modelling risk from a disease in time and space. *Statistics in Medicine*, 17(18), 2045–2060.

Lawson, A. and Lee, D. (2017). Bayesian disease mapping for public health. In *Handbook of Statistics*, volume 36, pages 443–481. Elsevier.

Lawson, A. B. (2001). Tutorial in biostatistics: Disease map reconstruction. *Statistics in Medicine*, 20, 2183–2203.

Lawson, A. B., Browne, W. J. and Vidal-Rodiero, C. L. (2009). *Bayesian Disease Mapping. Hierarchical Modeling in Spatial Epidemiology.* Chapman and Hall/CRC press, New York.

Lawson, A. B., Browne, W. J. and Vidal-Rodiero, C. L. (2013). *Bayesian Disease Mapping. Hierarchical Modeling in Spatial Epidemiology*. Chapman and Hall/CRC press, New York.

Lee, D. (2011). A comparison of conditional autoregressive models used in bayesian disease mapping. *Spatial and Spatio-temporal Epidemiology*, 2(2), 79–89.

Leroux, B. G., Lei, X. and Breslow, N. (1999). Estimation of disease rates in small areas: A new mixed model for spatial dependence. In *Statistical models in epidemiology, the environment and clinical trials.*, pages 135–178, New York, 1999. Springer-Verlag.

Lindgren, F. and Rue, H. (2015). Bayesian spatial modelling with r-inla. *Journal of Statistical Software*, 63(1), 1–25.

MacNab, Y. C. (2003). Hierarchical bayesian modeling of spatially correlated health service outcome and utilization rates. *Biometrics*, 59, 305–316.

MacNab, Y. C. (2007). Spline smoothing in bayesian disease mapping. *Environmetrics*, 18, 727–744.

MacNab, Y. C. (2011). On gaussian markov random fields and bayesian disease mapping. *Statistical Methods in Medical Research*, 20, 49–68.

MacNab, Y. C. (2014). On identification in bayesian disease mapping and ecological-spatial regression models. *Statistical Methods in Medical Research*, 23(2), 134–155.

MacNab, Y. C. and Dean, C. B. (2000). Parametric bootstrap and penalized quasi-likelihood inference in conditional autoregressive models. *PubMed: 10960863*, 19, 2421–2435.

MacNab, Y. C. and Dean, C. B. (2001). Autoregressive spatial smoothing and temporal spline smoothing for mapping rates. *Biometrics*, 57, 949–956.

MacNab, Y. C. and Gustafson, P. (2007). Regression b-spline smoothing in bayesian disease mapping: with an application to patient safety surveillance. *Statistics in Medicine*, 26, 4455–4474.

Martino, S. and Rue, H. (2009). *Implementing approximate Bayesian inference using integrated nested Laplace approximation: A manual for the inla program*. Department of Mathematical Sciences, Norway.

Molenberghs, G., Verbeke, G. and Demétrio, G. (2007). An extended random-effects approach to modeling repeated, overdispersed count data. *Lifetime Data Anal*, 13, 513–31.

Molenberghs, G., Verbeke, G., Demétrio, G. and Vieira, A. (2010). A family of generalized linear models for repeated measures with normal and conjugate random effects. *Stat Sci*, 25, 325–47.

NASCOP (2009). *Kenya AIDS Indicator Survey 2007: Final Report*. National AIDS and STI Control Programme, Nairobi, NASCOP.

NASCOP (2014). *Kenya AIDS Indicator Survey 2012: Final Report.* National AIDS and STI Control Programme, Nairobi, NASCOP.

NASCOP, KNBS and MOH (2017). *Kenya Demographic & Health Survey 2016*. Rockville, MD, USA: Kenya National Bureau of Statistics, Ministry of Health/Kenya, National AIDS Control Council/Kenya and ICF International.

Nathoo, F. S. and Ghosh, P. (2012). Skew-elliptical spatial random effect modeling for areal data with application to mapping health utilization rates. *Statistics in Medicine*.

Neyens, T., Faes, C. and Molenberghs, G. (2012). A generalized poisson-gamma model for spatially overdispersed data. *Spatial and Spatio-temporal Epidemiology*, 3, 185–194.

Ngesa, O., Achia, T. and Mwambi, H. (2014). A flexible random effects distribution in disease mapping models. *South African Statistical Journal*, 48(1), 83–93.

Ntzoufras, I. (2011). *Bayesian modeling using WinBUGS*, volume 698. John Wiley & Sons, Hoboken; New Jersey.

Palacios, M. (2006). Non-gaussian bayesian geostatistical modeling. *Journal of the American Statistical Association*, 101, 604–618.

Rampaso, R., de Souza, A. D. P. and Flores, E. (2016). Bayesian analysis of spatial data using different variance and neighbourhood structures. *Journal of Statistical Computation and Simulation*, 86(3), 535–552.

R Core Team (2016). *R: A language and environment for statistical computing. R Foundation for Statistical Computing*. MRC Biostatistics Unit, Austria.

Richardson, S. (2003). Spatialmodels in epidemiological applications. In Green, P., Hjort, N. and Richardson, S., editors, *Highly Structured Stochastic Systems*, pages 237–259. Oxford Statistical Science Series, UK.

Richardson, S., Thomson, A. and Best, N. a. (2004). Interpreting posterior relative risk estimates in disease-mapping studies. *Environ Health Pesp*, 112, 1016–1025.

Riebler, A., Sørbye, S. H., Simpson, D. and Rue, H. (2016). An intuitive bayesian spatial model for disease mapping that accounts for scaling. *Statistical Methods in Medical Research*, 25(4), 1145–1165.

Robert, C. and Casella, G. (2005). *Monte Carlo Statistical Methods*. Springer, New York, 2nd edition.

Rue, H. and Held, L. (2005). *Gaussian Markov random fields: theory and applications*. CRC Press, London.

Rue, H. and Martino, S. (2007). Approximate bayesian inference for hierarchical gaussian markov random field models. *J Stat Plan Inference*, 137, 3177–3192.

Rue, H., Martino, S. and Chopin, N. (2009). Approximate bayesian inference for latent gaussian models by using integrated nested laplace approximations. *Journal of the Royal Statistical Society, Series B*, 71, 319–392.

Sahu, S., Dey, D. and Branco, M. (2003). A new class of multivariate skew distributions with applications to bayesian regression models. *Canadian Journal of Statistics*, 31, 129–150.

Schrödle, B. and Held, L. (2011a). A primer on disease mapping and ecological regression using inla. *Computation Stat*, 26(2), 241–258.

Schrödle, B. and Held, L. (2011b). Spatio-temporal disease mapping using inla. *Environmetrics*, 22, 725–734.

Schrödle, B., Held, L. and Riebler, A. (2011). Using integrated nested laplace approximations for the evaluation of veterinary surveillance data from switzerland: a case-study. *Journal of the Royal Statistical Society, Series C*, 60, 261–279.

Sherman, M. (2011). *Spatial Statistics and Spatio-Temporal Data: Covariance Functions and Directional Properties*. Wiley, UK.

Spiegelhalter, D., Best, N., Carlin, B. and van der Linde, A. (2002). Bayesian measures of model complexity and fit (with discussion). *Journal of the Royal Statistical Society: Series B (Statistical Methodology)*, 64(4), 583–639.

Spiegelhalter, D., Thomas, A., Best, N. and Lunn, D. (2007). *WinBUGS User Manual, Version 1.4.3*. MRC Biostatistics Unit, UK.

Tierney, L. and Kadane, J. B. (1986). Accurate approximations fo posterior moments and marginal densities. *J Am Stat Assoc*, 81, 82–86.

Ugarte, M. D., Adin, A., Goicoa, T. and Militino, A. F. (2014). On fitting spatiotemporal disease mapping models using approximate bayesian inference. *Stat Methods Med Res*, 23(6), 507–530.

Ugarte, M. D., Adin, A., Goicoa, T. and Militino, A. F. (2017). One-dimensional, two-dimensional, and three dimensional b-splines to specify space–time interactions in bayesian disease mapping: Model fitting and model identifiability. *Spatial Statistics*, 22, 451–468.

Ugarte, M. D., Goicoa, T. and Etxeberrı´a, J. (2012a). A p-spline anova type model in space-time disease mapping. *Stoch Env Res Risk A*, 26, 835–845.

Ugarte, M. D., Goicoa, T. and Etxeberrı´a, J. (2012b). Projections of cancer mortality risks using spatio-temporal p–spline models. *Stat Methods Med Res*, 21, 545–560.

Ugarte, M. D., Goicoa, T. and Ibáñez, B. et al. (2009a). Evaluating the performance of spatio-temporal bayesian models in disease mapping. *Environmetrics*, 20, 647–665.

Ugarte, M. D., Goicoa, T. and Militino, A. F. (2009b). Empirical bayes and fully bayes procedures to detect high risk areas in disease mapping. *Comput Stat Data Anal*, 53, 2938–2949.

Ugarte, M. D., Goicoa, T. and Militino, A. F. (2010). Spatio-temporal modeling of mortality risks using penalized splines. *Environmetrics*, 21, 270–289.

Wakefield, J. (2007). Disease mapping and spatial regression with count data. *Biostatistics*, 8(2), 158–183.

Waller, L. A. and Gotway, C. A. (2004). *Applied Spatial Statistics for Public Health Data*, volume 368. John Wiley & Sons, Hoboken, New Jersey.

Wolpert, R. and Ickstadt, K. (1998). Poisson gamma random field models for spatial statistics. *Biometrika*, 85, 251–67.

APPENDICES

Appendix 1: RR estimates for the 2016 HIV and AIDS in Kenya

	PG		PLN		CON		pCARCOM		STCAR		STCARCOM	
node	mean	sd	mean	sd	mean	sd	mean	sd	mean	sd	mean	sd
RR[1]	0.9549	0.0098	0.9547	0.0099	0.9547	0.0099	0.9544	0.01	0.9543	0.0097	0.9545	0.01
RR[2]	0.2971	0.0038	0.2972	0.0038	0.2971	0.0039	0.2971	0.0039	0.2972	0.0038	0.2971	0.0039
RR[3]	0.0897	0.0044	0.0895	0.0044	0.0894	0.0044	0.0896	0.0044	0.0898	0.0044	0.0898	0.0044
RR[4]	0.0525	0.0016	0.0525	0.0016	0.0526	0.0017	0.0526	0.0016	0.0526	0.0016	0.0525	0.0016
RR[5]	0.3627	0.0043	0.3626	0.0043	0.3629	0.0044	0.3626	0.0043	0.3627	0.0043	0.3627	0.0044
RR[6]	0.5176	0.0044	0.5178	0.0044	0.5177	0.0043	0.5178	0.0044	0.5178	0.0043	0.5179	0.0043
RR[7]	0.7821	0.005	0.7821	0.0049	0.7819	0.0049	0.7821	0.0049	0.7821	0.0047	0.7822	0.005
RR[8]	0.3889	0.0043	0.389	0.0044	0.3889	0.0043	0.389	0.0042	0.3891	0.0043	0.3889	0.0044
RR[9]	0.4654	0.0019	0.4654	0.0019	0.4653	0.0019	0.4654	0.0019	0.4654	0.0019	0.4654	0.0018
RR[10]	1.243	0.0055	1.243	0.0054	1.243	0.0055	1.243	0.0053	1.243	0.0053	1.243	0.0053
RR[11]	0.6203	0.0051	0.6203	0.0051	0.6205	0.0051	0.6205	0.0051	0.6206	0.0052	0.6205	0.0051
RR[12]	0.1114	0.002	0.1114	0.0019	0.1114	0.002	0.1115	0.0019	0.1116	0.002	0.1115	0.0019
RR[13]	1.127	0.0136	1.127	0.0134	1.127	0.0135	1.128	0.0137	1.127	0.0137	1.128	0.0139
RR[14]	0.8873	0.0105	0.8872	0.0104	0.8873	0.0104	0.8871	0.0104	0.8876	0.0104	0.8872	0.0102
RR[15]	0.7778	0.0041	0.778	0.0041	0.7779	0.0042	0.7778	0.0041	0.7777	0.0042	0.7779	0.0043
RR[16]	1.494	0.0152	1.494	0.0152	1.495	0.0147	1.494	0.0152	1.494	0.0152	1.494	0.0154
RR[17]	0.5964	0.0031	0.5964	0.0031	0.5965	0.0031	0.5965	0.0032	0.5965	0.0031	0.5965	0.003
RR[18]	0.5834	0.0043	0.5834	0.0044	0.5833	0.0043	0.5833	0.0043	0.5834	0.0042	0.5833	0.0043
RR[19]	5.259	0.0155	5.259	0.0157	5.259	0.0157	5.259	0.0157	5.259	0.0155	5.26	0.0157
RR[20]	0.9854	0.0056	0.9855	0.0056	0.9854	0.0054	0.9854	0.0055	0.9854	0.0054	0.9853	0.0055
RR[21]	1.057	0.0098	1.057	0.0098	1.057	0.01	1.057	0.0098	1.057	0.0098	1.057	0.0099
RR[22]	0.8498	0.009	0.8497	0.009	0.8501	0.0089	0.8495	0.009	0.8501	0.0088	0.85	0.009
RR[23]	0.7996	0.0049	0.7995	0.005	0.7996	0.0049	0.7997	0.0049	0.7996	0.0049	0.7997	0.0049
RR[24]	0.8279	0.0065	0.828	0.0065	0.828	0.0066	0.8281	0.0066	0.8282	0.0066	0.8281	0.0067
RR[25]	4.219	0.0143	4.219	0.0145	4.219	0.0142	4.219	0.014	4.219	0.014	4.219	0.014
RR[26]	0.7385	0.0063	0.7386	0.0062	0.7387	0.0062	0.7384	0.0065	0.7383	0.0062	0.7386	0.0063
RR[27]	0.3976	0.0061	0.3974	0.006	0.3977	0.0061	0.3977	0.0061	0.3977	0.0061	0.3975	0.006
RR[28]	1.116	0.0058	1.116	0.0058	1.116	0.0059	1.116	0.0057	1.116	0.0057	1.116	0.0058
RR[29]	0.6708	0.0049	0.6707	0.0049	0.6707	0.0048	0.6708	0.0048	0.6708	0.0049	0.6708	0.0048
RR[30]	0.686	0.0033	0.686	0.0033	0.686	0.0033	0.6861	0.0032	0.6861	0.0033	0.6861	0.0031
RR[31]	5.53	0.0215	5.53	0.0219	5.529	0.0218	5.53	0.0217	5.529	0.0213	5.529	0.0219
RR[32]	0.5923	0.0058	0.5921	0.0058	0.5921	0.0059	0.592	0.006	0.592	0.0058	0.592	0.0058
RR[33]	1.366	0.01	1.365	0.0098	1.365	0.0098	1.365	0.0101	1.366	0.0099	1.365	0.0098
RR[34]	0.7317	0.0051	0.7319	0.0051	0.7318	0.0051	0.732	0.005	0.7323	0.005	0.7319	0.0051
RR[35]	0.9897	0.0064	0.9897	0.0063	0.9897	0.0064	0.9897	0.0065	0.9897	0.0063	0.9897	0.0061
RR[36]	0.9003	0.0052	0.9001	0.0052	0.9002	0.0052	0.9002	0.0052	0.9002	0.0052	0.9	0.0052
RR[37]	3.032	0.0111	3.033	0.0108	3.032	0.0109	3.032	0.0111	3.033	0.011	3.032	0.0111
RR[38]	1.202	0.02	1.202	0.0204	1.201	0.0204	1.201	0.0201	1.202	0.0205	1.202	0.0207
RR[39]	0.9307	0.0051	0.9308	0.005	0.9308	0.0051	0.9306	0.0051	0.9308	0.0051	0.9308	0.0051
RR[40]	1.114	0.007	1.114	0.0071	1.114	0.007	1.114	0.007	1.114	0.0071	1.114	0.007
RR[41]	1.206	0.0088	1.206	0.009	1.206	0.0089	1.206	0.009	1.206	0.009	1.206	0.0091
RR[42]	1.042	0.0074	1.042	0.0073	1.042	0.0073	1.042	0.0072	1.042	0.0074	1.042	0.0073
RR[43]	0.7122	0.0085	0.7123	0.0085	0.7126	0.0087	0.7123	0.0086	0.7124	0.0085	0.7121	0.0083
RR[44]	0.9263	0.0076	0.9263	0.0076	0.9264	0.0076	0.9263	0.0077	0.9265	0.0076	0.9263	0.0077
RR[45]	1.284	0.009	1.285	0.0089	1.285	0.0092	1.285	0.0091	1.285	0.0093	1.284	0.009
RR[46]	1.204	0.0048	1.204	0.0048	1.204	0.0048	1.204	0.0049	1.204	0.0049	1.204	0.0048
RR[47]	1.357	0.0083	1.357	0.0084	1.357	0.0083	1.357	0.0085	1.357	0.0083	1.357	0.0084

Appendix 2: WinBugs code for Skew-t Model

```
# Model
model {
# Likelihood
for (i in 1 : N) {
y[i]  ~ dpois(mu[i])
log(mu[i]) <- log(E[i]) + beta0 + phi[i]
RR[i] <- exp(beta0+phi[i]) # Area-specific relative risk
phi[i]<-sqrt(1/eta[i])*(delta*abs(Z[i])+ v[i])
v[i]~dnorm(0,tau)
# skew variables:
eta[i]~dgamma(df,df)
Z[i]~dnorm(0,1)
smr[i] <- (y[i])/(E[i])
ypred[i] ~dpois(mu[i])
PPL[i] <- pow(ypred[i]-y[i],2)
}
mspe <- mean(PPL[])
# Other priors:
beta0 ~dnorm(0,1.0E-6)
tau  ~ dgamma(0.5, 0.0005) # prior on precision
variance<- 1/tau # variance
sigma <- sqrt(1 / tau) # standard deviation
df<-k/2
k~dexp(lambda.nu)I(2,)
lambda.nu<- 0.1
delta ~dnorm(0, 0.01)
}
# Data
# Initials
```

```
list(beta0=0, tau=1, k=2,  delta= -1,
v=c(0,0,0,0,0,0,0,0,0,0,0,0,0,0,0,0,0,0,0,0,
0,0,0,0,0,0,0,0,0,0,0,0,0,0,0,0,0,0,0,0,0,0,0,0,0,0,0),
Z=c(0,0,0,0,0,0,0,0,0,0,0,0,0,0,0,0,0,0,0,0,0,0,0,0,0,0,0,0,0,0,
0,0,0,0,0,0,0,0,0,0,0,0,0,0,0,0,0),
eta=c(1,1,1,1,1,1,1,1,1,1,1,1,1,1,1,1,1,1,1,1,1,1,1,1,1,1,1,1,1,1,
1,1,1,1,1,1,1,1,1,1,1,1,1,1,1,1,1),
ypred=c(1,1,1,1,1,1,1,1,1,1,1,1,1,1,1,1,1,1,1,1,1,1,1,1,1,1,1,1,1,1
1,1,1,1,1,1,1,1,1,1,1,1,1,1,1,1,1))
```

Appendix 3: WinBugs code for Skew-t Spatial Combined Random Effects Model

```
#Model
model{
#Likelihood
for (i in 1 :N) {
# Specifying the likelihood:
y[i] ~ dpois(mu[i])
log(mu[i])<-log(E[i])+log(theta[i])+beta0+phi[i]
RR[i] <- theta[i]*exp(beta0+phi[i])  # Area-specific relative risk
phi[i]<-(U[i])/(sqrt(eta[i]))
omega.U[i]<- delta*abs(Z[i])
M[i]<-1/E[i]
smr[i] <- (y[i])/(E[i])
ypred[i] ~dpois(mu[i])
PPL[i] <- pow(ypred[i]-y[i],2)
# skew variables:
eta[i]~dgamma(df,df)
Z[i]~dnorm(0,1)
# Overdispersion random effect:
theta[i] ~ dgamma(a,b)
}
cumsum[1] <- 0
for(i in 2:(N+1)) {
cumsum[i] <- sum(num[1:(i-1)])
}
for(k in 1 : sumNumNeigh) {
for(i in 1:N) {
pick[k,i] <- step(k - cumsum[i] - epsilon)  * step(cumsum[i+1] - k)
#  pick[k,i] = 1    if     cumsum[i] < k <= cumsum[i=1];  otherwise
}
```

```
C[k] <- sqrt(E[adj[k]] / inprod(E[], pick[k,]))    # weight for eac
}
epsilon <- 0.0001
mspe <- mean(PPL[])
# Proper CAR prior distribution for spatial random effects:
U[1:N] ~ car.proper(omega.U[], C[],adj[], num[], M[], prec, rho)
# Other priors:
beta0 ~dnorm(0,1.0E-6)
a~dexp(1)
b~dgamma(0.1,1)
prec~ dgamma(0.5, 0.0005)
sigma<- sqrt(1 / prec)
df<-K/2
K~dexp(lambda.nu)I(2,)
lambda.nu<- 0.1
delta ~dnorm(0, 0.01)
#gamma~dbeta(18,2)I(,0.99)
rho.min <- min.bound(C[], adj[], num[], M[])
rho.max <- max.bound(C[], adj[], num[], M[])
rho ~ dunif(rho.min, rho.max)
}
# Data
# Initials
list(beta0=0, a=1, b=1, prec = 1, K=2,  delta= -1, rho=0.1,
U=c(0,0,0,0,0,0,0,0,0,0,0,0,0,0,0,0,0,0,0,0,0,0,0,0,0,0,0,0,0,0,
0,0,0,0,0,0,0,0,0,0,0,0,0,0,0,0,0,0),
theta=c(0.5, 1.5, 0.3, 0.7, 2.5, 1.3, 0.5, 0.4, 0.3, 2.1, 3, 2.3, 0
0.4, 0.2, 0.3, 0.2, 0.3, 0.2, 1.2, 0.2, 0.6, 1.6, 1, 0.2, 0.8, 0.7)
Z=c(0,0,0,0,0,0,0,0,0,0,0,0,0,0,0,0,0,0,0,0,0,0,0,0,0,0,0,0,0,0,
0,0,0,0,0,0,0,0,0,0,0,0,0,0,0,0,0,0),
eta=c(1,1,1,1,1,1,1,1,1,1,1,1,1,1,1,1,1,1,1,1,1,1,1,1,1,1,1,1,1,1,
```

```
1,1,1,1,1,1,1,1,1,1,1,1,1,1,1,1,1),
ypred=c(1,1,1,1,1,1,1,1,1,1,1,1,1,1,1,1,1,1,1,1,1,1,1,1,1,1,1,1,1,1
1,1,1,1,1,1,1,1,1,1,1,1,1,1,1,1,1))
```

Appendix 4: `R-INLA` codes for Spatio-temporal Analysis of HIV and AIDS in Kenya

```
require(INLA)
inla.setOption(scale.model.default=FALSE)
require(splancs)
require(sp)
require(fields)
require(maptools)
require(lattice)
require(abind)
library(spdep)
data <- read.csv(paste(" ",sep=""))
kenya <- readShapePoly(paste("",sep=""))
S=47
T=4
y.vector <- as.vector(as.matrix(data[,2:5]))#by column
E.vector <- as.vector(as.matrix(data[,6:9]))#by column
year <- numeric(0)
for(i in 1:4){
year<- append(year,rep(i,dim(data)[1]))}
county <- as.factor(rep(data[,1],4))
data <- data.frame(y= y.vector, E=E.vector,
ID.area=as.numeric(county),ID.area1=as.numeric(county),
year=year,ID.year = year, ID.year1=year,
ID.area.year = seq(1,length(county)))
temp <- poly2nb(kenya)
nb2INLA("kenya.graph", temp)
Kenya.adj <- paste("",sep="")
H <- inla.read.graph(filename="kenya.graph")
# Temporal graph
D1 <- diff(diag(T),differences=1)
```

```
Q.gammaRW1 <- t(D1)%*%D1
D2 <- diff(diag(T),differences=2)
Q.gammaRW2 <- t(D2)%*%D2
Q.xi <- matrix(0, H$n, H$n)
for (i in 1:H$n){
Q.xi[i,i]=H$nnbs[[i]]
Q.xi[i,H$nbs[[i]]]=-1}
Q.Leroux <- diag(S)-Q.xi
names <- kenya$NAME
data.kenya <- attr(kenya, "data")
formula.ST1 <- y ~  f(ID.area,model="bym",graph=Kenya.adj) +
f(ID.year,model="rw2") + f(ID.year1,model="iid")
model.ST1 <- inla(formula.ST1,family="poisson",data=data,E=E,
control.predictor=list(compute=TRUE))
temporal.CAR <- lapply(model.ST1$marginals.random$ID.year,
function(X){marg <- inla.tmarginal(function(x) exp(x), X)
inla.emarginal(mean, marg)})
temporal.IID <- lapply(model.ST1$marginals.random$ID.year1,
function(X){marg <- inla.tmarginal(function(x) exp(x), X)
inla.emarginal(mean, marg)})
###########################
### Spacetime interactions
###########################
#Type I interaction and RW2 prior for time#
formula.intI <- y ~ f(ID.area, model="generic1",
Cmatrix= Q.Leroux, constr=TRUE,
hyper=list(prec=list(prior="loggamma", param=c(1,0.01)),
beta=list(prior="logitbeta", param=c(4,2))))+f(ID.year1,
model="iid", constr=TRUE,hyper=list(prec=list(prior="loggamma",
param=c(1,0.01))))+f(ID.year, model="rw2", constr=TRUE,
hyper=list(prec=list(prior="loggamma", param=c(1,0.00005))))+
```

```
f(ID.area.year, model="iid", constr=TRUE,
hyper=list(prec=list(prior="loggamma", param=c(1,0.00005))),
extraconstr=list(A=matrix(rep(1:T,S),1,S*T),e=0))
model.intI<-inla(formula.intI, family="poisson", data=data, E=E,
control.predictor=list(compute=TRUE,cdf=c(log(1))),
control.compute=list(dic=TRUE),
control.inla=list(strategy="laplace"))
#Type II interaction and RW2 prior for time #
R <- kronecker(Q.gammaRW2,diag(S))
r.def <- 2*S
A.constr <- kronecker(matrix(1,1,T),diag(S))

formula.intII <- y ~ f(ID.area, model="generic1",
Cmatrix= Q.Leroux, constr=TRUE,
hyper=list(prec=list(prior="loggamma", param=c(1,0.01)),
beta=list(prior="logitbeta", param=c(4,2))))+f(ID.year1,
model="iid",constr=TRUE,hyper=list(prec=list(prior="loggamma",
param=c(1,0.01))))+f(ID.year, model="rw2", constr=TRUE,
hyper=list(prec=list(prior="loggamma", param=c(1,0.00005))))+
f(ID.area.year,model="generic0", Cmatrix=R, constr=TRUE,
hyper=list(prec=list(prior="loggamma", param=c(1,0.00005))),
extraconstr=list(A=A.constr, e=rep(0,S)))
model.intII<-inla(formula.intII, family="poisson", data=data, E=E,
control.predictor=list(compute=TRUE,cdf=c(log(1))),
control.compute=list(dic=TRUE),
control.inla=list(strategy="laplace"))
# Type III interaction and RW2 prior for time#
R <- kronecker(diag(T),Q.xi)
r.def <- T
A.constr <- kronecker(diag(T),matrix(1,1,S))
formula.intIII <- y ~ f(ID.area, model="generic1",
```

```
Cmatrix= Q.Leroux, constr=TRUE,
hyper=list(prec=list(prior="loggamma", param=c(1,0.01)),
beta=list(prior="logitbeta", param=c(4,2))))+f(ID.year1,
model="iid", constr=TRUE,hyper=list(prec=list(prior="loggamma",
param=c(1,0.01))))+f(ID.year, model="rw2", constr=TRUE,
hyper=list(prec=list(prior="loggamma",
param=c(1,0.00005))))+f(ID.area.year, model="generic0",
Cmatrix=R, rankdef=r.def,constr=TRUE,
hyper=list(prec=list(prior="loggamma", param=c(1,0.00005))),
extraconstr=list(A=A.constr, e=rep(0,T)))
model.intIII<-inla(formula.intIII, family="poisson", data=data,
E=E,control.predictor=list(compute=TRUE,cdf=c(log(1))),
control.compute=list(dic=TRUE),
control.inla=list(strategy="laplace"))
#Type IV interaction and RW2 prior for time #
R <- kronecker(Q.gammaRW2,Q.xi)
r.def <- 2*S+T-2
A1 <- kronecker(matrix(1,1,T),diag(S))
A2 <- kronecker(diag(T),matrix(1,1,S))
A.constr <- rbind(A1,A2)
formula.intIV <- y ~ f(ID.area, model="generic1",
Cmatrix= Q.Leroux, constr=TRUE,
hyper=list(prec=list(prior="loggamma",param=c(1,0.01)),
beta=list(prior="logitbeta",param=c(4,2))))+
f(ID.year1, model="iid", constr=TRUE,
hyper=list(prec=list(prior="loggamma", param=c(1,0.01))))+
f(ID.year, model="rw2", constr=TRUE,
hyper=list(prec=list(prior="loggamma", param=c(1,0.00005))))+
f(ID.area.year, model="generic0", Cmatrix=R, rankdef=r.def,
constr=TRUE, hyper=list(prec=list(prior="loggamma",
param=c(1,0.00005))),extraconstr=list(A=A.constr, e=rep(0,S+T)))
```

```
model.intIV<-inla(formula.intIV, family="poisson", data=data, E=E,
control.predictor=list(compute=TRUE,cdf=c(log(1))),
control.compute=list(dic=TRUE),
control.inla=list(strategy="laplace"))
delta.intI <- data.frame(delta=model.intI$summary.random$
ID.area.year[,2],year=data$ID.year,ID.area=data$ID.area)
delta.intI.matrix <- matrix(delta.intI[,1], 47,4,byrow=FALSE)
rownames(delta.intI.matrix)<- delta.intI[1:47,3]
delta.intII <- data.frame(delta=model.intII$summary.random$
ID.area.year[,2],year=data$ID.year,ID.area=data$ID.area)
delta.intII.matrix <- matrix(delta.intII[,1], 47,4,byrow=FALSE)
rownames(delta.intII.matrix)<- delta.intII[1:47,3]
delta.intIII <- data.frame(delta=model.intIII$summary.random$
ID.area.year[,2],year=data$ID.year,ID.area=data$ID.area)
delta.intIII.matrix <- matrix(delta.intIII[,1], 47,4,byrow=FALSE)
rownames(delta.intIII.matrix)<- delta.intIII[1:47,3]
delta.intIV <- data.frame(delta=model.intIV$summary.random$
ID.area.year[,2],year=data$ID.year,ID.area=data$ID.area)
delta.intIV.matrix <- matrix(delta.intIV[,1], 47,4,byrow=FALSE)
rownames(delta.intIV.matrix)<- delta.intIV[1:47,3]
# Check the absence of spatial trend for (intI)
cutoff.interaction <- c(-1,-0.01,0.01,1)
delta.intI.factor <- data.frame(NAME=data.kenya$NAME)
for(i in 1:4){delta.factor.temp <- cut(delta.intI.matrix[,i],
breaks=cutoff.interaction,include.lowest=TRUE)
delta.intI.factor <- cbind(delta.intI.factor,delta.factor.temp)}
colnames(delta.intI.factor)<- c("NAME",seq(2013,2016))

# Check the absence of spatial trend for (intII)
delta.intII.factor <- data.frame(NAME=data.kenya$NAME)
for(i in 1:4){delta.factor.temp <- cut(delta.intII.matrix[,i],
```

```
breaks=cutoff.interaction,include.lowest=TRUE)
delta.intII.factor <- cbind(delta.intII.factor,delta.factor.temp)}
colnames(delta.intII.factor)<- c("NAME",seq(2013,2016))

# Check the absence of spatial trend (intIII)
delta.intIII.factor <- data.frame(NAME=data.kenya$NAME)
for(i in 1:4){delta.factor.temp <- cut(delta.intIII.matrix[,i],
breaks=cutoff.interaction,include.lowest=TRUE)
delta.intIII.factor <- cbind(delta.intIII.factor,delta.factor.temp)
colnames(delta.intIII.factor)<- c("NAME",seq(2013,2016))

# Check the  absence of Spatial trend (intIV)
delta.intIV.factor <- data.frame(NAME=data.kenya$NAME)
for(i in 1:4){delta.factor.temp <- cut(delta.intIV.matrix[,i],
breaks=cutoff.interaction,include.lowest=TRUE)
delta.intIV.factor <- cbind(delta.intIV.factor,delta.factor.temp)}
colnames(delta.intIV.factor)<- c("NAME",seq(2013,2016))
#################################################
# Spatio-temporal interaction: Type I Interaction
#################################################
attr(kenya, "data") <- data.frame(data.kenya,
intI=delta.intI.factor, intII=delta.intII.factor,
intIII=delta.intIII.factor,intIV=delta.intIV.factor)
trellis.par.set(axis.line=list(col=NA))
spplot(obj=kenya, zcol=c("intI.2013","intI.2014","intI.2015",
"intI.2016"), col.regions=gray(2.5:0.5/3),
names.attr=seq(2013,2016),main="")
###################################################
# Spatio-temporal interaction: Type II Interaction
###################################################
spplot(obj=kenya, zcol=c("intII.2013","intII.2014","intII.2015",
```

```
"intII.2016"), col.regions=gray(2.5:0.5/3),
names.attr=seq(2013,2016),main="")
####################################################
# Spatio-temporal interaction: Type III Interaction
####################################################
spplot(obj=kenya, zcol=c("intIII.2013","intIII.2014","intIII.2015",
"intIII.2016"), col.regions=gray(2.5:0.5/3),
names.attr=seq(2013,2016),main="")
###################################################
# Spatio-temporal interaction: Type IV Interaction
###################################################
spplot(obj=kenya, zcol=c("intIV.2013","intIV.2014","intIV.2015",
"intIV.2016"), col.regions=gray(2.5:0.5/3),
names.attr=seq(2013,2016),main="")
```

Appendix 5: List of Publications from the Thesis

1. **Tonui Benard Cheruiyot**, Mwalili Samuel, Wanjoya Anthony (2018). *A More Robust Random Effects Model for Disease Mapping*. American Journal of Theoretical and Applied Statistics. Vol. 7, No. 1, pp. 29-34. doi:0.11648/j.ajtas.20180701.14

2. **Tonui, B.**, Mwalili, S. and Wanjoya, A. (2018). *Spatio-Temporal Variation of HIV Infection in Kenya*. Open Journal of Statistics, 8, 811-830. https://doi.org/10.4236/ojs.2018.85053